UNIVERSITY OF TURKU

Characterisation of the role of TLNRD1 in vascular development and integrity in zebrafish

Institute of Biomedicine, MDP in Biomedical Sciences
Drug Discovery and Development
Master's Thesis

Author:
Bence Berki

Supervisor:
Docent Ilkka Paatero, PhD, University of Turku

31.8.2022
University of Turku

Master's thesis
Subject: Institute of Biomedicine, MDP in Biomedical Sciences, Drug Discovery and Development
Author: Bence Berki
Title: Characterisation of the role of TLNRD1 in vascular development and integrity in zebrafish
Supervisor: Docent Ilkka Paatero, PhD, University of Turku
Number of pages: 61
Date: 31.8.2022

Angiogenesis, the formation of new blood vessels from existing vasculature, is an essential process for vascular growth and blood vessel development. However, defective regulation and abnormalities of angiogenesis are present in multiple diseases, such as cancer, diabetes, arthritis, psoriasis and many others. Angiogenesis utilizes multiple mechanisms, such as sprouting of new veins, vascular remodelling, tumour mediated trans-differentiation and vascular mimicry. In this research project, we focus on sprouting angiogenesis, filopodia and interacting proteins, which aid in the process of angiogenesis.

Talin rod domain-containing protein 1 (TLNRD1) is a small protein which shares homology with a major cytoskeletal protein Talin. Especially the domains R7 and R8 of Talin are most similar with TLNRD1. However, when comparing the genes encoding these domains, the area encoding domains R7 and R8 has 11 exons, but the gene encoding TLNRD1 consists from one single exon. This indicates that *tlnrd1*-gene is conserved in evolution, which is common for many important genes in cellular functions. TLNRD1 shares also the ability to bind and bundle actin with regular Talin, which is necessary for filopodia formation and linked with sprouting angiogenesis. The goal of this research project was to shed light on this role of TLNRD1, by using a zebrafish model.

The common zebrafish (*Danio rerio*) is a vastly used animal model in vascular growth and cancer research. For this project, a transgenic strain of TLNRD1 mutant fish was produced prior the project, and all of the research was conducted with under 5-day old zebrafish embryos. First, embryos of TLNRD1-mutants were produced and imaged with a stereomicroscope for observing structural differences in their vasculature. The lengths and diameters of blood vessels were measured and analysed statistically. Genotyping was done with PCR and gel electrophoresis. Within the first two groups of naturally spawned embryos, no significant differences were observed between the control and mutant groups. Also, visual phenotype related observations of abnormalities or vasculature changes were quite minuscule.

In the second phase of the experiment, a set of microinjections with CRISPR-CAS9 and single guide RNAs were done, to find out how the gene edition of TLNRD1 effects on the phenotype. A new set of embryos were injected within one hour of fertilization, and they were observed for 3 days, after which imaging and data analysis was done again. Due to using CRISPR for gene editing, instead of regular genotyping a T7 endonuclease assay was conducted to measure the gene edition. In addition, a database search of RNA expression patters of TLNRD1 was conducted with using the UCSC Cell Browser and a high-profile transcriptional RNA dataset of zebrafish. The conclusion of this project was that although TLNRD1 has previously been shown to affect vascular development, no major significance or visual phenotype differences were observed among the target embryos. Possible reasons could be the somewhat low levels of initial expression of TLNRD1 or the actual significance of the protein being smaller in vascular development than previously anticipated. More research about the thesis topic would be needed to develop the knowledge about TLNRD1.

Keywords: angiogenesis, zebrafish, protein analysis, microinjection, CRISP-CAS9

Table of Contents

1 Introduction

1.1 Vascular system

Vascular growth is one of the most essential processes during embryo development. The vasculature system is among the first developing organ systems originating from the mesodermal embryonic layer, developing from mesodermal stem cells, which mature further to hemangioblasts. These cells will branch in development either in the direction of hematopoietic stem cells (HSCs) or angioblasts. (Schmidt *et al.* 2007, Risau 1997)

The role of vascular development is to form new blood vessels, and up keep the vasculature system. The major role of the system itself is to deliver oxygen, nutrients and metabolite molecules for different cells and tissues. The system also transports wastes away from tissues, delivering them to their respective organs such as the liver, kidneys etc. (Tucker *et al.* 2021)

All blood vessels beside the cardiac veins, are a part of the peripheral vascular system. The blood vessels within the circulatory system are divided further in arterioles, capillaries, venules and veins. Generally, blood vessels have three distinct layers, tunica adventia (outer layer), tunica media (middle layer) and tunica intima (inner layer). (Taylor & Bordoni 2022) The adventia is the major structure and support provider for the vessels. The nerves that are connected to the outer layer membrane cells, are also part of the adventia. With the aid of collagen junctions and elastic fibres, vascular endothelial cadherin (VE-Cadherin) and tight junction protein 1 (ZO-1), the adventia attaches the vessel in the surrounding tissue. (Welti *et al.* 2013)

The tunica media is the vascular smooth muscle cell layer below the adventia. It alters the size of the lumen by contraction and relaxation. The layer also consists from elastin and collagen (Cronenwett & Johnston 2014). In the arterioles, tunica media is thicker compared to the venules, where it is rather thin. (Taylor & Bordoni 2022) This correlates with the arteries having higher blood pressure in them compared to the venules. (Cronenwett & Johnston 2014)

The tunica intima is the last layer before the vessel lumen, and it consists from a simple squamous endothelial cell layer. The layer is connected through the basal lamina to the extra cellular matrix (ECM). The epithelial layer of tunica intima is interacting with the blood plasma and all the cells circulating in the lumen. (Taylor & Bordoni 2022)

Arteries transport highly oxygenated blood from the heart and distribute it all around the body delivering also nutrients to the tissues. The larger arteries (aorta, pulmonary veins, branchial, radial and femoral arteries) have elastic and muscular layers to provide support and to hold the higher blood pressure. When moving towards the target tissues, the arteries branch into smaller arterioles. The arterioles play an important role in systemic vascular resistance which is regulated by the autonomic nervous system. Thus, the blood pressure stays in balance when the supporting tunica adventia and tunica media shrink in size towards the capillaries. (Tucker *et al.* 2021)

Capillaries are the smallest units of the vasculature system. They have a simple cellular wall consisting from the basal lamina, single layer of flattened endothelial cells and pericytes. The pericytes are neurologically active vascular signalling cells, which respond to changes in the blood pressure. In the capillary level, exchange of oxygen and nutrition molecules is happening by diffusion, and the flow of blood is regulated by the arteriolar lumen. (Taylor & Bordoni 2022)

Capillaries can also be divided into smaller subtypes, which are continuous capillaries, fenestrated capillaries and discontinuous capillaries. The continuous capillaries are the most common type, mainly present in muscle tissues, connective tissues, skin, lungs and the central nervous system (CNS). They have a continuous basal lamina, which wraps around the endothelial layer, which has small pores for transcytosis. Fenestrated capillaries have circular fenestrations in the endothelia and their basal lamina is continuous. This feature is essential in the endocrinal organs and absorptive tissues such as the intestinal tract, kidneys and the pancreas. The discontinuous capillaries are present in tissues where large amounts of blood passes through. These tissues inclue the liver, spleen and the bone marrow where hepatocytes are produced. Discontinuous capillaries have large fenestrated epithelial layers with gaps both between the endothelial cells (ECs) but also in the basal lamina. (Taylor & Bordoni 2022)

Venules are the continuation from capillaries on the way back to the heart, where low oxygenated blood flows after the red blood cells and target tissues exchange oxygen to carbon dioxide. The structure of the venules includes the basal lamina, endothelial cells and pericytes, but fewer subendothelial fibres compared to capillaries. The tunica medina of venules consists from one to two layers of vascular smooth muscle cells. (Taylor & Bordoni 2022) The other distinctive feature of venules is the post-capillary sphincters which prevent the backwards flow of the blood. (Tucker *et al.* 2021)

Venules continue to widen into larger veins closer to the heart. Among the veins, the tunica media and tunica adventia are much thinner than in arteries. The small to medium size veins have more vascular smooth muscle cells in their tunica media, than the larger veins which replace the larger muscle layer with connective tissue. Since the lumen in veins is wider, the majority of the blood volume is residing in the veins, during the circulatory cycle. Veins also have generally lower blood pressure, due to looser wall structure. (Pugsley & Tabrizchi 2000)

1.2 Vascular growth types

When considering vascular growth, there are two major types of development. Blood vessel development from individual stem cells called vasculogenesis and branching growth of new vessels from pre-existing vasculature called angiogenesis. Tumour mediated angiogenesis is also committing to vascular development in e.g. cancers. (Udan *et al.* 2012)

1.2.1 Vasculogenesis

In the embryonal state, blood vessel formation is progressing through vasculogenesis, where the progenitor cells of the new blood vessel are derived from individual endothelial cells (ECs). The ECs originate from angioblasts. The pericytes surrounding the blood vessels develop from mesenchymal stem cells (MSCs). (Wong & Crawford 2013). The process occurs in three steps. First the fibroblast growth factors (FGF) are introduced to the hemangioblasts. This initiates the formation of the first chords of developing vessels. Next the vascular endothelial growth factor (VEGF) mediates the merging and assembly of the progenitor vessels. The expression of receptor proteins for FGF, VEGF and other angiogenic licands, profiles the vasculogenesis to proceed towards angiogenesis (Wang & Zhao 2010). Multiple growth factors, morphogens and other signalling molecules aid to modulate the vascular development further. (Adair & Montani 2010)

In adults the process of vasculogenesis is functioning differently. The pericytes originate from fibroblasts, which reside in the bone marrow, and the ECs are derived from endothelial progenitor cells (EPCs). The EPCs form structures called the blood islands, clusters of HSCs and angioblasts, in the mesoderm. The HSCs develop further into hematopoietic blood cells and angioblasts develop into endothelial cells which are migrating to compose a new blood vessel. (Lugano *et al.* 2020)

The process of vasculogenesis in adults occurs mostly whenever the vascular tissue encounters damage, such as in case of post ischemia (Asahara *et al.* 1997), hypoxia progressing to anoxia (Krock *et al.* 2011) and would healing (Wong & Crawford 2013) where cytokines and other hypoxia related signalling pathways activate and recruit EPCs to the damaged tissue site.

1.2.2 Angiogenesis

Angiogenesis occurs mainly in two ways, which are sprouting angiogenesis and intussusceptive angiogenesis aka. vascular remodelling. Angiogenesis is present in normal vascular development and also in tissue healing (Li *et al.* 2003), organ regeneration (Jahani *et al.* 2020) and tumour genesis (Zhao *et al.* 2011).

Sprouting angiogenesis takes place in the blood vessel ECs, which are activated by proangiogenic molecules such as VEGF, and together by alterations in the cell-cell junctions and interactions with the basal lamina, the process of tip cell formation is initiated (Welti *et al.* 2013). The outmost vascular EC develops into the outward sprouting "tip cell" which begins to migrate away from the vascular endothelia towards the surrounding ECM. The front of the tip cell forms the filopodia structure, a cytoplasmic extension of the lamellipodium. The role of the filopodia is to aid the cell in probing the surrounding ECM and directing the tip cell migration. The structure is composed mostly from cytoskeletal proteins e.g. F-actin (Phng *et al.* 2013). The following ECs behind the tip cells develop into vastly proliferating stalk cells, which follow the migrating tip cell and continue elongating the branching vessel's body. Although the order of the migrating cells is tip cells first, followed by the stalk cells, the phenotype of the vascular ECs is fluid, meaning the rates of proangiogenic factors are regulating the profiling of cells either into tip cell or stalk cell directions. (Welti *et al.* 2013) Pathways that take part in this controlling include e.g. the Notch signalling pathway (Potente *et al.* 2011) and the Wnt pathway (Olsen *et al.* 2017).

Migration of tip cells is following the extracellular VEGF gradient. The direction of the cell adhesion is also mediated by integrins (Arvaamides *et al.* 2008), and signalling molecules like ephrins (Kujiper *et al.* 2007) and semaphorins (Basile *et al.* 2004). When two different migrating tip cells encounter, they merge together in a process called anastomosis, which is aided by macrophages and myeloid cells. The macrophages interact with the opposing tip cell filopodia and clump in the site of anastomosis. The merging forms a connection between the sprouting vessels.

The proliferating stalk cells are simultaneously elongating the sprouting vein. The formation of basal lamina and recruiting pericyte precursor cells by platelet derived growth factor (PDGF) establishes the base for the new stabile lumen. The stabilization of the new vein is further aided by Ve-cadherin, ZO-1 with EC junctions, pericyte maturation and finally the presence of blood flow in the new lumen. (Carmeliet & Jain 2011)

Intussusceptive angiogenesis forms new veins by dividing existing vessels into two separate lumens and remodelling them into new entities. The exact mechanism of intussusception is not entirely known, so some of the mechanisms explained below are presumptive. The first phase of intussusception includes the development of various infoldings and protrusions in the vascular endothelia wall. This process is considered to be faster and less reliable on direct EC proliferation than sprouting angiogenesis. (Burri *et al*. 2004)

In sites of intussusception, often the most common noticeable feature are transluminal pillars, which extend into the lumen of the blood vessel. They are interacting with firmly packed collagen fibres, which are clothed by ECs. These structures, are shown to have a lack of any other types of cells, like pericytes, and the ECs surrounding the collagen fibres lack also the basal lamina. However, the ECs of the pillars contain high electron density areas which indicate adhesion sites being present between the collagens and the ECs. These sites also show to contain certain attachment points, rich in vinculin, which aids the collagen to bundle and pull the pillar into the existing vessel lumen. (Paku *et al.* 2011)

Integrins are also noticed to be present in these transluminal pillars, e.g. integrin α-1 and β-2, especially in more maturated pillars. The role of the integrins may be debatable, demonstrated in the case of Paku *et al.* 2011, because of the low levels of integrin expression. However, integrins have been proven to aid cell adhesion and have an effect on the contractive properties of the actomyosin cytoskeleton (Meshel *et al.* 2005) which is linked with angiogenesis. The maturation of transluminal pillars leads to vessel separation and it can happen by one or multiple simultaneous pillars migrating and changing the vascular morphology. (Makanya *et al.* 2009)

The transluminal pillars grow by time, affecting on vascular remodelling and at least three outcomes in vascular morphology and function of intussusception are proposed. These are microvascular growth, arborization and branching remodelling. The microvascular growth is necessary for the capillary plexus's expansion, which is essential in capillary bed formation of

various organs. Intussusceptive arborization is needed for development of supplying blood vessels for the capillary plexus. This happens by transforming regions of the capillaries to arterioles or by collecting vessels and altering their size and orientation. The branching remodelling is a process to optimize the vascular three and the effective blood flow within pre-and postcapillary vessels. (Dojov *et al.* 2003)

1.2.3 Vasculogenic mimicry

One of the mechanisms of angiogenesis related to cancers is the vascular channel formation by tumour cells aka. vasculogenic mimicry. The blood vessels are formed from tumour tissue instead of proliferating EPCs and the cancer mimics the vascular structure (Maniotis *et al.* 1999). Vasculogenic mimicry is often associated with aggressive invasive cancers with high grades of tumours, quick metastasis and poor prognosis among patients with malignant tumours. The process of angiogenesis by tumours is complex and multiple effector proteins and cells such as VEGF, FGF, matrix metalloproteinases (MMPs), macrophages and fibroblasts aid the tumour-controlled angiogenesis (Luo *et al.* 2020). In order to vasculogenic mimicry to happen, highly malignant tumours, adaptor molecules and growth factors are needed to degrade or remodel the ECM, leading to the formation of vessel-like structures which are connected to existing blood vessels (Maniotis *et al.* 2002). Vasculogenic mimicry can occur by two mechanisms, which are either tubular type of vessel formation or patterned matrix type of vessel formation.

In the tubular type, blood vessels are formed from tumour cells which assemble in tubular structures connected to glycoproteins. The tubular formation can be initiated by inadequate blood flow present in tumours. The development of tumour cells to mimic ECs is reinforced by pro-angiogenic factors essential for cancer proliferation. In glioblastoma cells, such factors include epidermal growth factor receptors (EGFR) and gene expression of endothelium related genes including ephrin type-A receptor 2 (EphA2), Laminin subunit gamma-2 (LAMC2) and Neuropilin 2 (NRP2) (El Hallani *et al.* 2010). The patterned matrix type of vasculogenic mimicry requires tumour cells and different ECM associated proteins like laminin, proteoglycans and collagens (type IV and type VI), which help to wrap the cells and the proteins together forming a matrix pattern. (Ayala-Domínguez *et al.* 2019) Specifically this type of vessel formation does not correspond neither to tubular nor common structural formations of blood vessels.

1.2.4 Tumour mediated trans-differentiation

The neovascularization caused by tumours may occur also in the form of trans-differentiation, in which cancer cells differentiate into ECs or endothelial smooth muscle cells. This way of blood vessel formation has been reported to be present in various cancer types and cells e.g. glioblastoma cells (Ricci-Vitiani *et al.* 2010), human breast (Bussolati *et al.* 2009) and ovarian cancer cells (Alvero *et al.* 2009). One of the major suggested reasons for tumour mediated endothelia trans differentiation is the expression of the Twist Family BHLH Transcription Factor 1 (Twist1). The phosphorylation of the Ser42 residue of Twist1, results in promotion of the expression of angiopoietin-1 receptor (TIE2), which has an important role between the ECs and the surrounding ECM. (Mammoto *et al.* 2016). Twist1 also regulates the expression of other prior listed pro-angiogenic factors such as the PDGF and the receptor complex type 2 of VEGF (VEGFR2). However, in some cases the trans-differentiation of tumour cells is considered to be debatable, since in clinical data, the genetic alterations of ECs in patients with glioblastoma tumours, do not seem to match with the genetic profile of the other metastatic cancer cells. (Rodriguez *et al.* 2012 & Kulla *et al.* 2003)

The emerged forms of abnormalities in tumour related angiogenesis has also promoted the research of therapeutically potential targets for anti-angiogenetic and antitumoral treatments related to blood vessel formations. (Ge & Luo 2018)

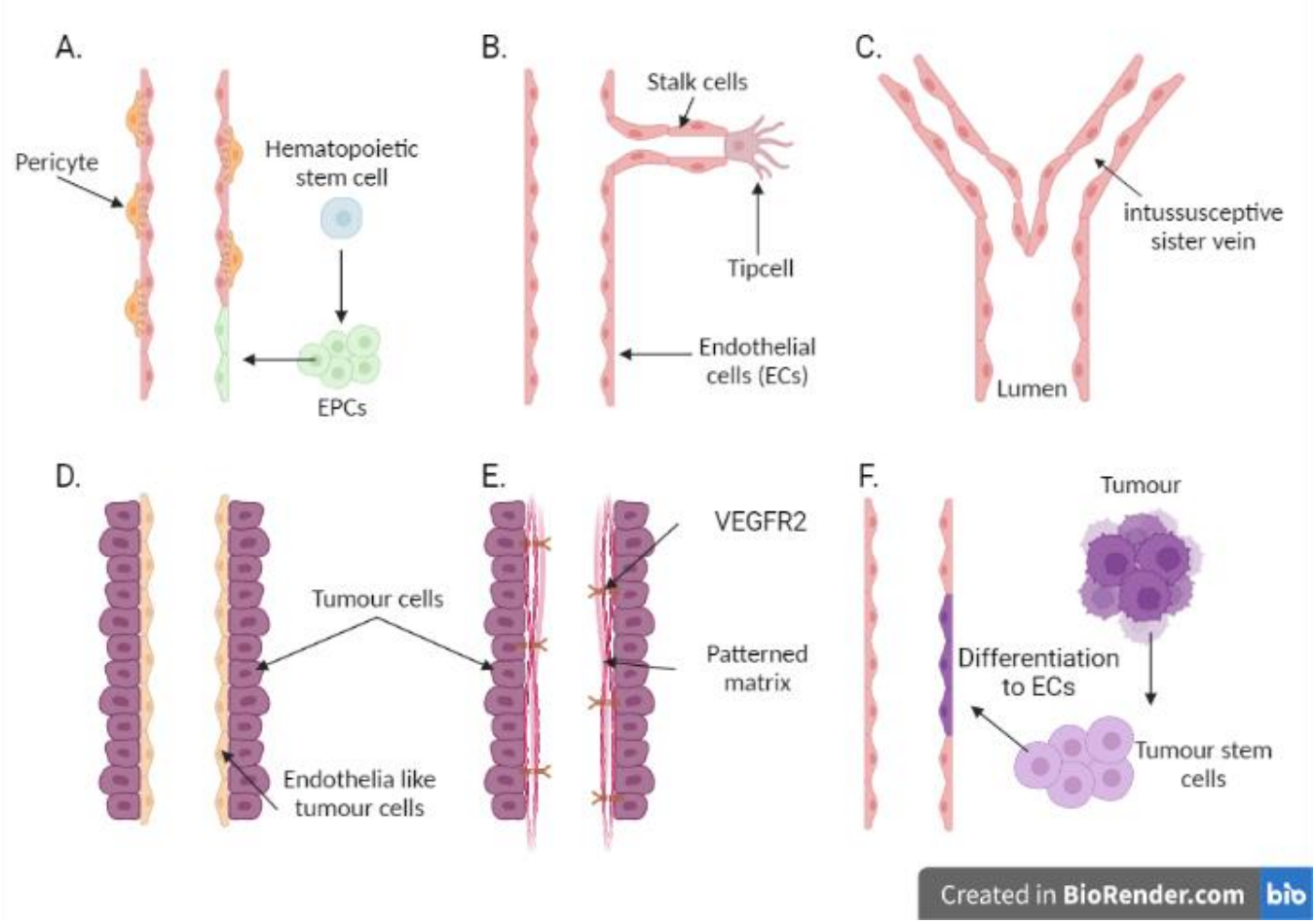

Figure 1. – A simplified image of the different mechanisms of vascular growth. A) Vasculogenesis, the development of ECs from stem cells, B) Sprouting angiogenesis, the formation of new blood vessels by cell proliferation and migration, C) intussusceptive angiogenesis, morphological changes in pre-existing veins, D) Vasculogenic mimicry of tumour cells (tubular type formation), E) Vascular mimicry of tumour cells (with a patterned protein matrix structure) and F) Tumour mediated trans differentiation of tumour cells turning into blood vessel ECs. (Berki 2022, Image created with Biorender.com)

1.3 Major effectors of vascular growth and development

As previously stated, angiogenesis is a complex process that is possible via multiple mechanisms and various different effectors and pathways that are related to vascular development. In this section we break down more the individual roles of these effectors and pathways.

1.3.1 VEGF

Vascular endothelial growth factor (VEGF) is a family of mitogen proteins, which have the key role in embryonal and postnatal angiogenesis. The protein is encoded by one gene, but due to alternative splicing, the protein has multiple isoforms. (Neufeld *et al*. 1999) The first discovered isoform was the $VEGF_{165}$ (Ferrara & Henzel 1989), which has been later classified in the group of VEGF-A proteins. VEGF has been conserved through evolution for quite a long time, although species like fish and mammals have been separated from their common ancestors over 450 million years ago. Still, roughly 60-69% of the amino acid sequences of the VEGF proteins for respective species share identical similarity (Gong *et al.* 2004). In total by this date seven members of the VEGF family have been discovered: VEGF-A, VEGF-B, VEGF-C and VEGF-D which appear in human cells and are responsible in lymphatic development, placental growth factor (PIGF) (Ferrara 2004), Orf virus-derived VEGF-E (Ogawa *et al.* 1998) and snake venom derived VEGF-F (Yamazaki *et al.* 2009).

Among these types of VEGF, VEGF-A emerges as the most prevalent effector on angiogenesis, and thus it is among the most studied proteins of the family. All of the VEGF proteins are secreted proteins and they appear mainly in endothelial tissues, fibroblasts, alongside tumours, macrophages, platelets and keratinocytes and smooth muscle cells. (Peach *et al.* 2018)

The vascular endothelial growth factor receptors (VEGFRs) are a type IV receptor tyrosine kinases (RTK), which have three subtypes of VEGFRs. VEGFR1 which is encoded by the gene *Flt1* orthologue, VEGFR2 encoded by the gene *kdr*, and VEGFR3 which is encoded by the gene *Flt4* orthologue. (Koch *et al.* 2011)

VEGFR1 is roughly 180-185 kDa size transmembrane glycoprotein, which is most expressed in ECs, monocytes, macrophages, vascular smooth muscle cells and renal mesangial cells. In

addition, a soluble subtype for VEGFR1 has been characterised, called sVEGFR1, which lacks the subcellular tyrosine kinase domain of the receptor. (Barleon *et al.* 2001)

Primarily the binding ligand for VEGFR1 is VEGF-B, but the receptor has affinity towards VEGF-A and PIGF as well. The binding of these ligands causes two monomers of VEGFR1 to form a dimeric structure, through the Ig-like D7 membrane proximal domain (Yang *et al.* 2010). The dimerisation initiates trans- and autophosphorylation of the tyrosine kinase domains leading to downstream cell signalling. The effects of these signalling pathways include multiple suggested processes. One is the activation of JAK/STAT partially in hypoxic conditions, which is associated with cell proliferation (Bellik *et al.* 2005). The regulation of chemotaxis in monocytes via downstream tyrosine kinase receptors such as ERK, MAPK, PI3K and NFAT1 has been associated with cell migration and angiogenesis (Ding *et al.* 2010 & Tchaikovski *et al.* 2008). Also, the VEGFR1 related initiation of PI3K/Akt activation has been linked with the EC differentiation and development into vascular tubes (Cai *et al.* 2003)

VEGFR2 is a 210-230 kDa glycoprotein, the primary receptor binding VEGF-A, but it also has the ability to bind proteolytically edited variations of VEGF-C and VEGF-D. Like VEGFR1, it has soluble version of the receptor, but VEGFR2 also can form trans membranal heterodimers with VEGFR1 and VEGFR3 *in vitro*. (Huang *et al.* 2001 & Dixelius *et al.* 2003) VEGFR2 is endemic in the vascular ECs with strong expression in other cells like the retinal progenitor cells and HSCs. The expression of VEGFR2 is conjoined with angiogenesis and tumour related neovascularization. (Koch *et al.* 2011) The activation of the VEGFR2 takes place after VEGF-A binding to the extra cellular domains, which initiates the phosphorylation of several tyrosine sites resulting in activation of the vast network of downstream cell signalling pathways.

Phosphorylation of Tyr951 results in the activation of T-cell specific adaptor protein (TSAd), which activates the proto-oncogene tyrosine protein kinase (SRC) pathway. This leads to the regression of VE-cadherin bound endothelial junctions (Sun *et al.* 2012). The phosphorylation of Tyr1175 effects on activation of phospholipase Cγ (PLCγ) mediated ERK1/2 signalling, which is necessary in EC proliferation and development (Takahashi *et al.* 2001). The same residue effects also on the recruitment of SH2 domain containing adaptor protein B (SHB), which is needed together with focal adhesion kinase (FAK) to initiate filopodia formation and cell migration (Abu-Ghazaleh *et al.* 2001). The Tyr1175 activation also effects on the signal transducer IQ-motif-

containing GTPase activating protein 1 (IQGAP1) which is required for binding actin filaments, which are essential in cell-cell junctions, proliferation and cell adhesion. (Yamaoka-Tojo *et al.* 2006) It has been also suggested, that VEGFR2 dependent activation of scaffold adapter Gab1, results to the downstream signalling via PI3K in the phosphorylation of protein kinase B (Akt) which also phosphorylates apoptosis affiliated proteins like BAD and caspase 9, resulting in inhibition of apoptosis and prolonging cell survival. (Shimotake *et al.* 2010)

VEGFR3 is the final known VEGF receptor type. The protein is secreted as a 195 kDa precursor protein, which is proteolytically cleaved from the 5th extracellular domain, creating a disulphide bonded N-terminal peptide. The receptor can form homodimer structures by itself and heterodimeric structures with VEGRF2. The receptor is primarily expressed during embryogenesis in vein ECs but also in the direction of embryonal lymph genesis. (Kaipainen *et al.* 1995 & Tammela *et al.* 2008) The activation of VEGFR3's tyrosine residues Tyr1230 and Tyr 1231 is affecting on similar signalling pathways discussed previously, ERK1/2 and Akt via PI3K which are needed both in lymph genesis and angiogenesis. (Mäkinen *et al.* 2001) The phosphorylation of multiple tyrosine residues (especially Tyr830, Tyr833, Tyr853, Tyr1063, Tyr1333 and Tyr1337) has been linked with independent activation of VEGRF3 signalling pathways by different integrins. The interaction with ECM collagen I binding with integrin β1, recruits the cellular adaptor protein SRC to phosphorylate the respective tyrosine residues. This activates other downward signalling adaptors like CRKI/II and SHC which regulate the Jun N-terminal kinase pathway (JNK). JNK is a commonly mitogen associated signalling pathway, which is related to cellular proliferation, adhesion and cell survival. (Galvagni *et al.* 2010)

1.3.2 PDGF

The platelet derived growth factors are a group of mesenchymal originating adaptor proteins, which have important functions related to cellular growth, survival and adhesion. The PDGF family consists from 4 isoforms A-D, which form homodimers and one heterodimer AB via disulphide bonding. The respective tyrosine kinase receptors for these polypeptides are either PDGFR-α or PDGFR-β or the intermediate heterodimer PDGFR-αβ containing both monomers of the receptor type. The activation of ligand binding initiates phosphorylation of tyrosine sites of the receptors effecting on multiple cellular signalling pathways already mentioned such as SRC, ERK, PI3K, PLCγ and JAK/STAT. (Heldin 2013)

In angiogenesis, PDGF has a role in stabilization of vessel maturation, by vascular ECs releasing PDGF-B chemo gradient, which lures pericytes with PDGFR-β to strengthen the blood vessels, vascular tubes and also activating mural cells. In cases of PDGFR inhibition, tumour related vascular growth is supressed and the lack of detached pericytes creates vessel leakages and vessel deformation. (Bergers *et al.* 2003) The blocking of PDGF-B therapeutically has been suggested to be one way of treating pulmonary hypertension and malformations in the vasculature. (Lebrin *et al.* 2010)

1.3.3 FGF

The fibroblast growth factor superfamily (FGF) is a group of mitogenic growth factors. There are 18 in total of them, ranging from FGF1-FGF10 to FGF16-FGF23. These paracrine factors have been linked with embryonal tissue development, organ and tissue patterning and cell growth, especially among the five first subfamilies of FGF (Itoh & Ornitz 2004). The excluded family including FGF19, FGF21 and FGF23 have been shown to work more as endocrines in the regulation of bile acids, cholesterol, glucose and vitamin D with the aid of klotho proteins associated with diseases such as diabetes type two (Kharitonenkov *et al*. 2005).

FGF1, FGF2 and FGF4 have been associated with angiogenesis and cardiac events. Similarly, to VEGFR, the genes encoding FGFRs are spliced alternatively in their mRNA stage, which results in four types of FGFR, from FGFR1 to FGFR4. FGFR1 is showcasing the broadest range of expression patterns among the four receptors and it has seven known tyrosine sites that lead to down stream cell signal activation (Klint & Claesson-Welsh 1999).

It has been noticed that in rats, FGF1 and FGF2 lower blood pressure when administered and this results in normalisation of hypertension and increased amount of nitric oxide synthase enzymes in vascular ECs (Cuevas *et al.* 1996). The downstream signalling by the autophosphorylation of FGFR1 includes SHC (Klint *et al.*1999), CRK (Larsson *et al.* 1999), PLCγ (Mohammadi *et al.* 1991) and MAPK (Larsson *et al.* 1999). The expression of protein kinase C (PKC) is also essential for achieving the complete response of FGF2 in ECs (Kanno *et al.* 2000). The signalling of these pathways is connected to EC proliferation, adhesion, maturation and cellular survival, which all are needed for angiogenetic development.

1.3.4 TGF-β

Transforming growth factor beta (TGF-β) is a group of cytokines part of a protein family affecting on various cellular functions such as growth, proliferation and cellular differentiation. The cytokine is also associated with different cancers. (Kubiczkova *et al.* 2012)

TGF-β effects are driven by the ligands, from which three isoforms have been characterised (TGF-β1, TGF-β2 and TGF-β3) which bind to two types of transmembrane receptors TGF-βR1 and TGF-βR2. The ligand binds to TGF-βR2, which leads to heterodimerisation of TGF-βR1 and TGF-βR2, initiating the downstream cell signalling. (Massagué 1998) This signalling can happen via small Mothers against Decapentaplegic (SMAD) pathway or via non-SMAD related pathways like P13K, Ras/Raf activated ERK1/2 (Liu *et al.* 2018) or MMP regulated epithelial mesenchymal transition (EMT) (Yu & Stamencovic 2000).

When looking into the angiogenic properties of TGF-β, the cytokine is considered to be a proangiogenic factor, due to increased protein levels in tumour vasculature in non-small lung carcinomas (Hasegawa *et al.* 2001). In breast cancer, the possibility to form osteolytic metastasis is strongly related to overexpression of interleukin-11 and connective tissue growth factor (CTGF). The expression of these factors is also enhanced by TGF-β, resulting in multiple functions essential for metastasis, one of them being tumour angiogenesis (Kang *et al.* 2003). It has been also reported that together with the hypoxia-inducible factor (HIF-1), TGF- β is contributing positively to angiogenesis promotion via VEGF related gene expression with presence of SMADs and HIF-1 (Sánchez-Elsner *et al.* 2001).

However, Geng et al. proves that the TGF-β and HIF-1 related pathway also supresses VEGF-A expression and thus angiogenesis in certain cancers, trough ubiquitination and protein degradation. The suggested pathway for this is the SMAD3/PKA pathway (Geng *et al.* 2013). The role of TGF-β as an angiogenetic promoter is also debated in the study by Jarad et al. where the cytokine seemed to have both pro and anti-angiogenic properties simultaneously. Which direction the mediator leans, depends on the dominantly expressed pathway being either ALK5/SMAD2 mediated or TGF-β/ALK1 mediated. The inhibition with TFG-β resulted in promoted expression of endoglin and reduced signalling via Notch1 and VEGFR2 reducing sprouting angiogenesis. (Jarad *et al.* 2017)

1.3.5 HIF-1

When tissues undergo high stress or oxygen depletion, which is enhanced with disrupted oxygenation, the physiological state of hypoxia is created. Hypoxia is associated often with cardiovascular diseases, pulmonary events, different cancers and the expression of hypoxia mediated transcription factors contribute to neovascularisation and angiogenesis (Bárdos & Ashcroft 2005).

The heterodimeric transcription factor hypoxia-inducible factor 1 (HIF-1) is the key mediator in hypoxia response and oxygen balance regulation. The two subunits making up HIF-1, HIF1-α and HIF-1β, share both structural similarities with their basic helix loop helix (bHLH) domain and the Per-Arnt-Sim (PAS) domain (Wang *et al.* 1995). The HIF1-α subunit has in addition an oxygen dependent degradation (ODD) domain, which is hydroxylated by proline-hydroxylase-2 (PHD2) and recognized by von Hippel-Lindau (VHL) ubiquitin ligase complexes. In normal conditions when oxygen is available, HIF1-α is prone to degradation by proteasomes (Huang *et al.* 1998). In hypoxic conditions however, the lack of oxygen reduces both PHD2 and VHL functions, allowing HIF1-α to dimerize with the HIF1-β subunit. The transactivation domain of the c-terminal (TADC) of HIF1-α acts as binding region for two co-activators called CREB binding protein (CBP) and p300 (Lando *et al.* 2002). These co-activators aid in HIF-1 mediated gene expression leading to upregulation of various factors such as erythropoietin, glucose transporters, glycolytic enzymes and VEGF (Pagé *et al.* 2002). The increase of VEGF expression initiates neovascularisation in hypoxic tissues and commits positively to vascular EC proliferation as well (Carmeliet *et al.* 1998).

Since HIF-1 expression promotes angiogenesis and circulation, it has been a target for treatment in ischemic conditions. Especially the increase of HIF1-α levels in blood have been noticed to decrease ischemic cell damage in cardiomyocytes and the reaction level of myocardial infarction in murine hearts is diminished when HIF1-α is overexpressed (Date *et al.* 2005 & Kido *et al.* 2005). Although HIF-1 is associated with neovascularization, and in cardiovascular events and ischemia, they may provide therapeutically aid, the relation of HIF-1 with cancers is somewhat problematic. This is due to neovascularisation and tumour angiogenesis being present also in several cancers and HIF-1 is strongly related with poor prognosis in e.g. colorectal cancer. (Baba *et al.* 2010)

1.3.6 Angiopoietins and integrins

Tyrosine kinases with immunoglobulin and EGF like domains 1 and 2 (TIE1 and TIE2) are members of the tyrosine kinase receptor proteins, which act as angiopoietin receptors in endothelial cells. The most researched angiopoietins type 1 and 2 (ANG1 and ANG2) are required in vascular maturation and remodelling and their role is tied with vascular endothelial homeostasis, inflammation and angiogenesis (Eklund & Saharinen 2013).

The ANG-TIE pathway functions as a unique pathway for both allocating TIE receptors in EC-EC junctions or interacting with EC-ECM contacts. Primarily the binding of ANG1 mediates the formation of TIE1-TIE2 receptor complex which results in trans activation of two receptor complexes in an EC-EC junction. The activation also effects on further downstream cell signalling by activation of Akt and Dok-R docking protein pathways present in cellular migration (Saharinen *et al.* 2008).

The role of ANG2 is much dependent on the vascular microenvironment, due to the simultaneous antagonist / agonist nature for TIE2. The excess amount of ANG2 can reduce cell-cell phosphorylation in the EC-junctions and thus promoting vasculature stability and EC permeability, while ANG1 activation does the opposite (Saharinen *et al.* 2008).

However, it has been noticed that different types of integrins act also receptors for angiopoietins, both in ECs but also in other cells, such as ovary, adrenal medulla, astrocytes and retinal cells. The presence of ANG1 promotes focal adhesion kinase (FAK) signalling via binding to integrin $\alpha_v\beta_5$, which promotes the recruitment of fibronectin for filopodia formation and branching angiogenesis (Lee *et al.* 2013).

ANG2 activates β1-integrin, which is needed in EC cellular junctions and ECM connections. This indicates that ANG-TIE related signalling is needed also in promoting of cellular adhesion in angiogenesis, both for tip cell migration and filopodia formation. The localization of TIE2 receptors in cellular junctions seemingly promoted cytoskeletal changes, ECM adhesion and reduction of cell to cell junction integrity in ANG2 transgenic mice (Hakanpää *et al.* 2015).

1.4 Talin and cell adhesion

In order for branching angiogenesis to happen, the filopodia in focal adhesion sites is needed to direct the cells migration in the ECM. Talin, a 270 kDa sized cell adhesion protein, plays an important role in the formation of filopodia and how it is connected to the cytoskeleton. The protein consists of two distinct main domains, the 47 kDa head domain and the 210 kDa Talin rod domain. The two domains are interlinked together with a 9 kDa linker region which elongates the protein by 20 nm and includes a site for protease cleavage. (Bate *et al.* 2012)

The head domain of talin consists from a common subcellular plasma membrane linking FERM-domain (four-point-one, ezrin, radixin, moesin), which has the typical F1, F2 and F3 subdomains. Compared to regular FERM-proteins, the talin head also has a specific F0 domain. The F3 domain has a direct site for β-integrin binding, and the other domains F1 and F2 have positively charged amino acid residues, which interact with the negatively charged membrane phospholipids. The process is needed for integrin activation and integrin clustering. (Elliot *et al.* 2010) The F0-domain role is still researched, but it is suggested that it acts as a helper and stabilizing factor for the FERM-domain in order to link talin with integrins (Gingras *et al.* 2019).

Talin rod domain is made up from 13 subdomains (R1-R13), which are all groups of alpha helixes. The domains consist from 4-5 helixes, which form tight bundles with hydrophobic centres. Most of the domains are positioned in a line, but the R8 helix bundle is positioned into a loop between the helixes of the R7 domain. This differently positioned R7R8 bundle is the main link between talin, the cytoskeleton and integrins (Goult *et al.* 2018).

The rod subdomains have multiple binding cites for different cell adhesion and cytoskeletal proteins, like vinculin, F-actin, Rap-1-GTP-interacting adaptor protein (RIAM) and Rho GTPase activating protein 7. The sites for binding vinculin especially are interestingly cryptic, which means that they become available only when the subdomains of talin rod encounter unfolding. This happens whenever cell adhesion takes place or as a response of gradual force. The binding of vinculin has been seen to induce downstream signalling pathways which mechanically strengthen the cellular adhesion (del Rio *et al.* 2009).

Regularly in cells with no signal for adhesion, talin is folded in the inactive form. Talin is activated together by the phosphoinositol-4,5-bisphosphate (PIP2) and GTPase-Rap1/RIAM pathways.

PIP2 attracts the talin head domain to connect with the plasma membrane, with a push-pull technique and the RIAM-RAP1 protein complex binds to the talin rod subdomains specifically the domains R2 and R3 but also R8 and R11. The difference compared to vinculin however is that RIAM binds only to folded R2 and R3 talin domains, while vinculin binds only to unfolded R-domains (Goult *et al.* 2013). The R7 domain of talin has been reported to also bind KANK1 protein, in formation of cortical microtubule formations related to focal adhesions (Bouchet *et al.* 2016).

The force induced unfolding of talin rod subdomains results, in possible vinculin and integrin interactions. When talin is actively bound to transmembrane integrins, and activated by RIAM, the binding of vinculin leads to actin filament recruitment in the focal adhesions. Vinculin acts as a bridge between plasma membrane bound talin via integrins, and actin filaments are bound to vinculin, forming a connection to the cytoskeleton. The stronger talin activation is expressed, the higher adhesion turnover rate occurs, and the stronger cellular adhesion is taking place (Yang *et al.* 2014 & Rahikainen *et al.* 2017).

1.5 Talin rod domain-containing protein 1

In 2021, Cowell *et al.* published a paper about the small protein called talin rod domain containing protein 1 (TLNRD1) and how it is related to the cytoplasm adaptor protein talin and filopodia formation. The gene encoding TLNRD1 was originally discovered in the human chromosome 15 within the mesd locus, and due to this it was named to mesoderm development candidate 1 (MESDC1), which is used at times when referring to TLNRD1 (Cowell *et al.* 2021).

TLNRD1 is a small (approx. 37 kDa) helical protein, consisting of two helical domains, with 9 alpha helixes in total, 5 helixes housing both the N- and C-terminus and a distinguished 4 helix domain. The 4-helix domain is placed between the helixes α3 and α8 of the 1st domain, and they are connected via a loop structure. In the crystal structure of TLNRD1, the protein forms an antiparallel dimer structure. TLNRD1 shares homology with talin domains R7 and R8, with 22 % identical amino acid sequence (Cowell *et al.* 2021).

Interestingly enough, the gene encoding TLNRD1 consists from one singular exon region, while the talin domains R7 and R8 are encoded by a gene that has 11 exons. Singular exon genes are often associated with features that are conserved in evolution, meaning the genes do not under go

as much changes as other regions of the genome. Upon conducting a phylogenetic evolutive analysis, TLNRD1 seems to be present in vertebrates and other animal phyla including Echinoderms, Lophotrochozoa, Sponges and Choanoflagellates. The gene is not present in Nematodes, Arthropods and Cnidaria. This indicates that TLNRD1 has some important role in cellular functions through different groups of Animalia, which is supporting the importance of evolutive conservation (Cowell *et al.* 2021).

TLNRD1 has both structural and functional similarity with the R7 and R8 domains of talin. They both can bind actin and LD-motif including adaptor proteins such as RIAM and KANK. Although TLNRD1 does not have the vinculin binding sites, the role of TLNRD1 has been associated with talin modulation, through a dominant negative regulator which may detach talin R7R8 domains from integrins (Cowell *et al.* 2021).

It is also reported that TLNRD1 has a potential oncogenic function within bladder cancer cell lines, and the tumour suppressor microRNA miR-574-3p bounds to the *tlnrd1*-gene inhibiting cell proliferation and tumour invasion (Tatarano *et al.* 2012).

The dimerization of TLNRD1 has been shown to promote actin localization and bundling, and thus because actin binding proteins have been shown to promote filopodia formation (Khurana & George 2011), TLNRD1 has been associated with it as well. And as earlier established, filopodia being an important structure in several cell adhesive processes, and it is present in cancer and branching angiogenesis, the exact function of TLNRD1 in filopodia formation could provide new information and aspects for angiogenesis and cell adhesion research.

1.6 Zebrafish and angiogenesis

Zebrafish (*Danio rerio*) have been emerged as a promising *in vivo* model organism for vasculature research (Chávez *et al.* 2016), due to their relative fast development larval stage, large number of offspring and relatively cohesive profile of molecularly similar pathways with vertebrates. The translation of zebrafish vascular biology with human vascular biology is backed up with both pharmacological and genetic evidence (Coultas *et al.* 2005).

Due to the transparent tissues of zebrafish embryos, the biomedical imagining of targets has been proven to be much convenient than for example murine models, with opaque and unavailable

vascular tissues without surgical procedures. Observations such as direct blood flow, live imaging of cardiac functions and overall embryonal development are possible to follow with mere microscopy (Chávez *et al.* 2016).

The genetic profile of zebrafish is also well known and characterized, which makes it also easy to edit with molecular biology tools like CRIPS-CAS9 and TALEN (Bendell *et al.* 2012). By the vast possibilities to edit transgenic zebrafish strains and develop different disease models, there are over 20 000 different transgenic strains available (Ruzicka *et al.* 2015). One of the most commonly applied transgenic feature for zebrafish embryos is the insertion of a fluorescent protein, which aids imaging various tissues and organs. Zebrafish can be also utilized as a xerographic cancer model. (Chávez *et al.* 2016)

One of the stand out features in zebrafish embryos and vascular development is the passive diffusion of oxygen in the embryonic stage, which allows the embryos to continue development even through with greater vascular malformations. With this, the observation of vascular deformations in late phenotypes makes it possible to research vasculature effects on certain genes. In mammals the deformed vasculature leads to lethal conditions in early embryonal stages. (Isogai *et al.* 2003)

Zebrafish models related to angiogenesis are most often focusing of vascular regeneration and sprouting angiogenesis. The areas where these processes are examined include the dorsal inter segmental vessels (ISV) and the dorsal aorta. The angiogenesis assays often include also dose dependent drug interactions, because the model makes it easy to culture embryos in different drug dilutions *ad libitum*. The application of drugs in the zebrafish models is present also in high throughput screening (HTS), which is essential in early stage drug development. With testing new components within zebrafish embryo cultures, the toxicity and possible effects on vasculature can be detected easily by phenotypical data. With this quick method, possible new drug molecules can be screened out early, if they result in increased numbers of deformations. (Chávez *et al.* 2016)

1.7 Summary

In conclusion, angiogenesis is a very complex and multiple factor mediated process, which is related to several different diseases. Multiple growth factors such as VEGF, PDGF, FGF, TGF-β, HIF-1, angiopoietins and cell adhesion mediators take a part in angiogenesis. The most often

utilized downstream signalling in angiogenesis is mediated by autophosphorylation of several receptor tyrosine kinases. Multiple other non-angiogenic cell processes also utilize these same pathways.

The research and further investigation of TLNRD1 may bring new perspectives and information related to cell adhesion research alongside with angiogenesis. The role of the small protein is still rather unclear. The evolutive conservation of TLNRD1 supports the theory that it is essential in neovascularisation and it is present in multiple distinct animal groups.

Zebrafish (*Danio rerio*) are a common model organism to research angiogenesis. The fast development cycle, large offspring numbers, transparency and easily editable genome are among the several reasons, why the model is utilized. Zebrafish are also a good animal model in early stage drug development, due to easy toxicity affirmations and easily translational genetic profile of the model.

1.8 Aims of the research

The goal of this study was to identify and characterise the proper role of TLNRD1 in regulation of vascular morphogenesis and vascular integrity. Our hypothesis for the project was that TLNRD1 affects angiogenesis in developing zebrafish embryos with a clearly visible phenotype. The mutated allele of *tlnrd1* was used mainly as a tool to answer our hypothesis. Upon concluding the thesis project, we hoped to have new insight of the function of TLNRD1 in vascular morphogenesis, vascular integrity and highlight the possible effect of gene edition on the gene with the aid of Crispr-Cas9. Obtaining information on the preliminary therapeutic potential of targeting TLNRD1 was also one of the goals of this study, although in the end it is only theorised in the discussion. The experiment was done by using a knockout zebrafish model with a mutant variation of *tlnrd1*. Genotypical and phenotypical data was compared between wild type embryos and the mutant embryos. Microinjections were performed afterwards with embryos with a wild type gene of *tlnrd1*, but the gene was edited using single guide RNAs and Crispr-Cas9 to see, if the interference to the gene causes visible vasculature changes. Physical parameters of the vasculature in the different sample groups were measured and satisficed.

2 Results

2.1 Visual phenotypes

The results are based on comparative observation between the naturally spawn embryo group and microinjected embryo group. Altogether 2 sets of normally recombined groups were spawned, and at least 4 sets of microinjected embryos. Unfortunately, not all of the obtained data was usable due to lack of clear phenotype or correct genotyping results. The overall data and results are based on the 2nd naturally spawned embryo group (mCherry-marked) and the 3rd and the 4th groups of microinjected embryos (eGFP marked).

First in order to obtain the embryos, adult zebrafish were mated in the specific mating tank, from which embryos were collected on a petri dish. The plates were screened post harvesting daily, to remove undeveloped and infertile eggs to avoid contamination of the samples. Within 5 days of fertilisation the embryos were imaged, using a fluorescence microscope. The transgenic fluorescent mCherry and eGFP proteins aided the visualisation of the vasculature of the embryos. The results of the naturally spawn embryos are presented below.

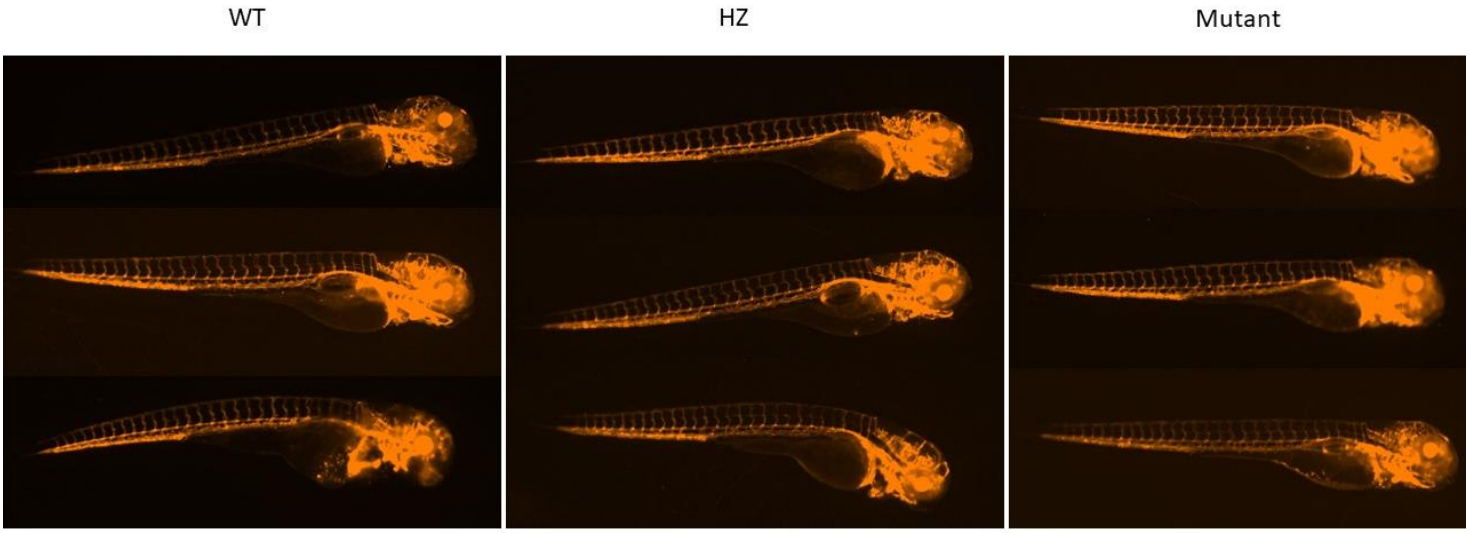

Figure 2. - A showcase of the 2nd normally produced embryo sample groups and the different genotypes within the group. Altogether 59 samples were imaged and measured. A notable feature is that there are no huge differences between the vasculature system of the genotypes. The only mention worthy difference is the "hunchback" phenomenon (in the bottom left and middle). This feature was present in at least 7/59 samples regardless of the genotype. However, the feature does not seem to affect the overall anatomy of the vasculature.

2.2 Genotyping

After imaging the fish, the embryos were placed in individual Eppendorf tubes for tissue lysis and DNA extraction. This was done in preparation for the genotyping of the embryos, to match the genotypic data, with the obtained visual phenotypic data from the fluorescence images. The end goal of the genotyping was to determine whether the genotype is affecting on the visible phenotype of the embryos, their vascular structure and integrity. Also, after the genotyping, the obtained rates and distribution of the genotypes within the sample group, aid to reveal how the *tlnrd1* is inherited and is there a possibility for one genotype to result in early development lethality. The genotyping was conducted with a two staged PCR assay, and the samples were analysed on an agarose gel electrophoresis. In total 59 samples were genotyped and the results of the genotyping rates are shown in Table 1 and the statistical analysis of the genotype distribution in Table 2. The genetic distribution was analysed with a Hardy-Weinberg chi-square test, to showcase if the observed data (genotypes) are equivalent to the expected data (Mendelian distribution meaning 1/4).

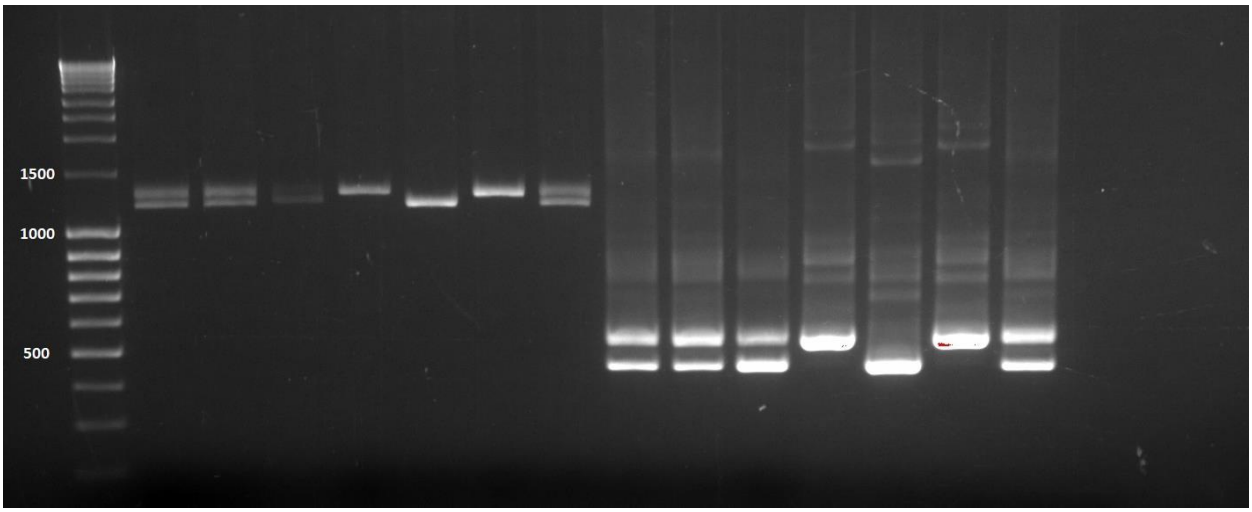

Figure 3. – Genotyping PCR and the resulting electrophoresis (in 2% agarose gel run in 100V for 1 hour). In this gel both steps of the genotyping PCR are visible. The wells from 1 to 7 are the 1st round of the PCR showing bands between 1500-1000 bp, and the following wells from 8 to 14 with bands near 500 bp are from the 2nd round, where the product of the 1st round is used as template DNA. The final well 15 is a negative water control. In the results 7 samples can be seen, from which 4 are Heterozygotes (double band), 2 mutants (only the upper band) and one wild type (only the lower band).

Table 1. - The distribution of the successfully genotyped samples in the 2nd group of normally spawn embryos

Sample size (N)	Wild type (WT)	Hetero Zygote (HZ)	Mutant (M)
59	13 (22%)	31 (53%)	15 (25%)

Table 2. – Hardy-Weinberg chi-square test for checking the genetic distribution of the tlnrd1-gene against the traditional mendelian distribution (WT = 1/4, HZ = 2/4 and M = ¼)

Hardy-Weinberg chi-square test for genetic distribution

	Observed N	Expected N	Residual
0	13	14,75	-1,7
1	31	29,50	1,5
2	15	14,75	0,3
Total	59		

Chi-square test

	Genotype
Chi-Square	0,288[a]
df	2
Asymp. Sig.	0,866

a. 0 cells (0,0%) have expected frequencies less than 5. The minimum expected cell frequency is 14,8.

2.3 Physical parameters of the vasculature

From the data obtained from the fluorescence imaging, three distinct parameters were measured. The overall body length of the embryos, width of the caudal vein (CV) which was the average of 3 measuring spots, and the widths of the dorsal inter segmental veins (ISV) which were the average of 5 measuring points. As discussed in the introduction, the signs of angiogenesis and vascular malformations are often observed best from these sites.

The measurements were done in the ImageJ processing software Fiji and are presented as µm. After measurements the results were charted, quantified and analysed statistically. The visuals of the statistical analysis from the 2nd naturally spawn embryo group are presented in Figure 4 and the statistical confirmation with a one-way-ANOVA test is shown in Table 3. Initially the sample size was 59, but due to the lack of fluorescent indicator in few embryos, the statistical data for the CV and ISV parameters is done with n = 46 samples. The body length was possible to measure from the bright field images with the initial sample size.

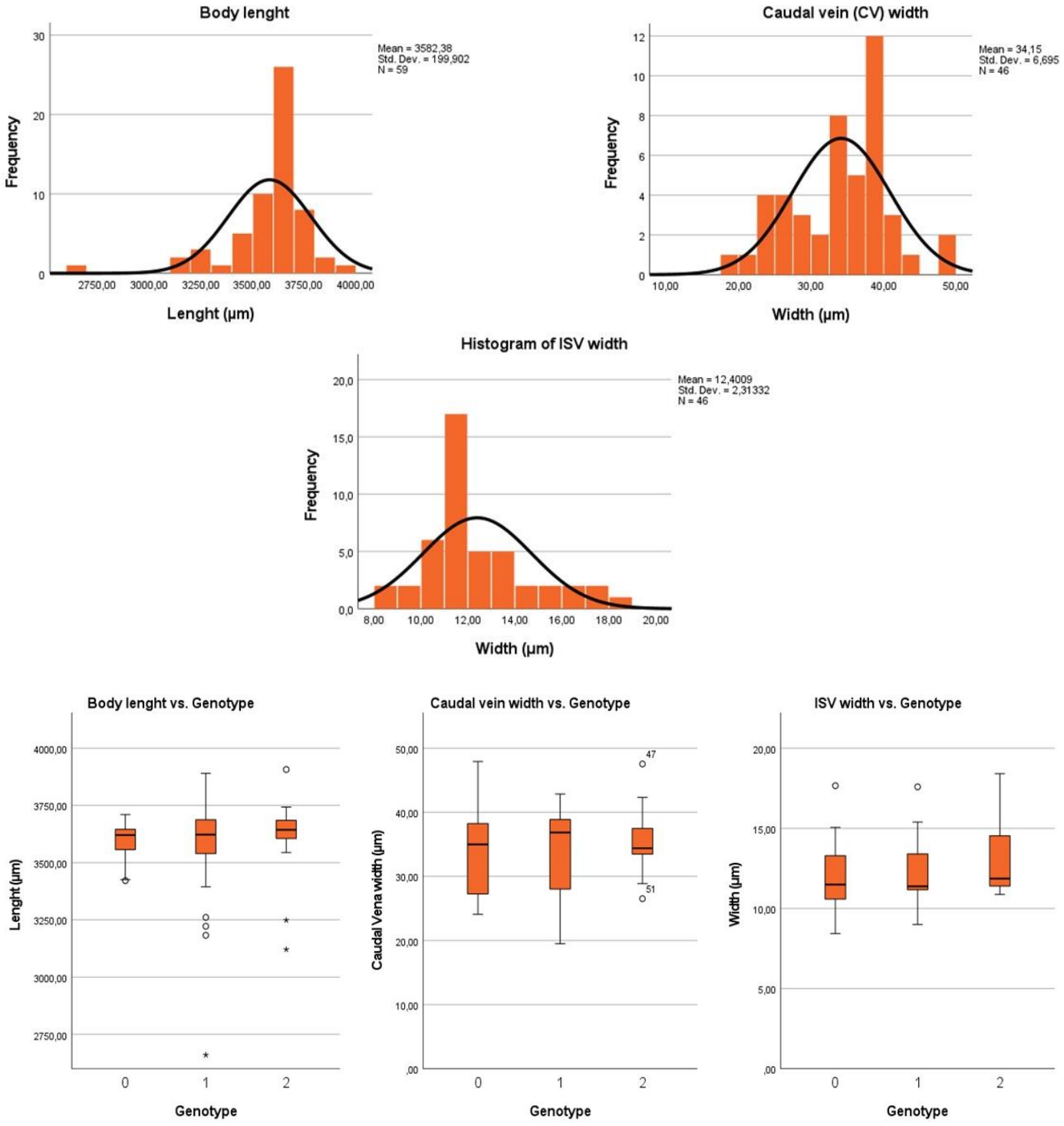

Figure 4. Statistical data of the regularly spawned embryos and the measured parameters. In the top of the figure, histograms showcase the body length, caudal vein and intersegmental vein widths in a normal distribution. Bottom row, the boxplots show the variation of these parameters regarding of the genotype of the samples. The genotypes are marked as 0 = WT, 1 = HZ and 2 = M.

Table 3. – One-way ANOVA test for normally spawned embryos

		Sum of Squares	df	Mean Square	F	Sig.
Body length	Between Groups	17413,985	2	8706,993	0,212	0,810
	Within Groups	2300310,529	56	41076,974		
	Total	2317724,514	58			
Caudal vein width	Between Groups	26,992	2	13,496	0,292	0,748
	Within Groups	1989,791	43	46,274		
	Total	2016,784	45			
Intersegmental vein width	Between Groups	7,910	2	3,955	0,730	0,488
	Within Groups	232,905	43	5,416		
	Total	240,815	45			

2.4 DNA sequences and RNA expression data

Among the genotyped PCR products, a few bands were sent to sequencing analysis, using the commercial sequencing services provided by Eurofins Scientific. This step of the project was done for figuring out does the mutated variant have larger scale edition in the *tlnrd1* gene.

All together 4 samples were sent for sequencing, two M-samples and two WT-samples of *tlnrd1*. After the sequencing the data was obtained online, and analysed with computational sequencing tools, trimming and aligning the sequences with BLAST. The alignment result is visualised in Figure 5.

As a part of the thesis project, for getting information of the genetic expression and how it is present in the different tissues of zebrafish embryos, an online database search was also conducted. By using the UCSC Cell Browser library from zebrafish (Farnsworth *et al.* 2020), information of the RNA expression rates of tlnrd1 were obtained. For comparison, the gene encoding talin (*tln1*) was also screened from the database. The results of visualising the expression patters are presented in Figure 6.

*Figure 5. DNA sequence of the TLNRD1 gene. A comparison and alignment of mutant (M = Contig1) and wild type (WT = Contig 2) forms of TLNRD1. The results show 97% in sequence similarity, with eight point-mutations (lack of *) and a 78 bp insertion in the mutated sequence between nucleotides 148 and 226 (red arrow).*

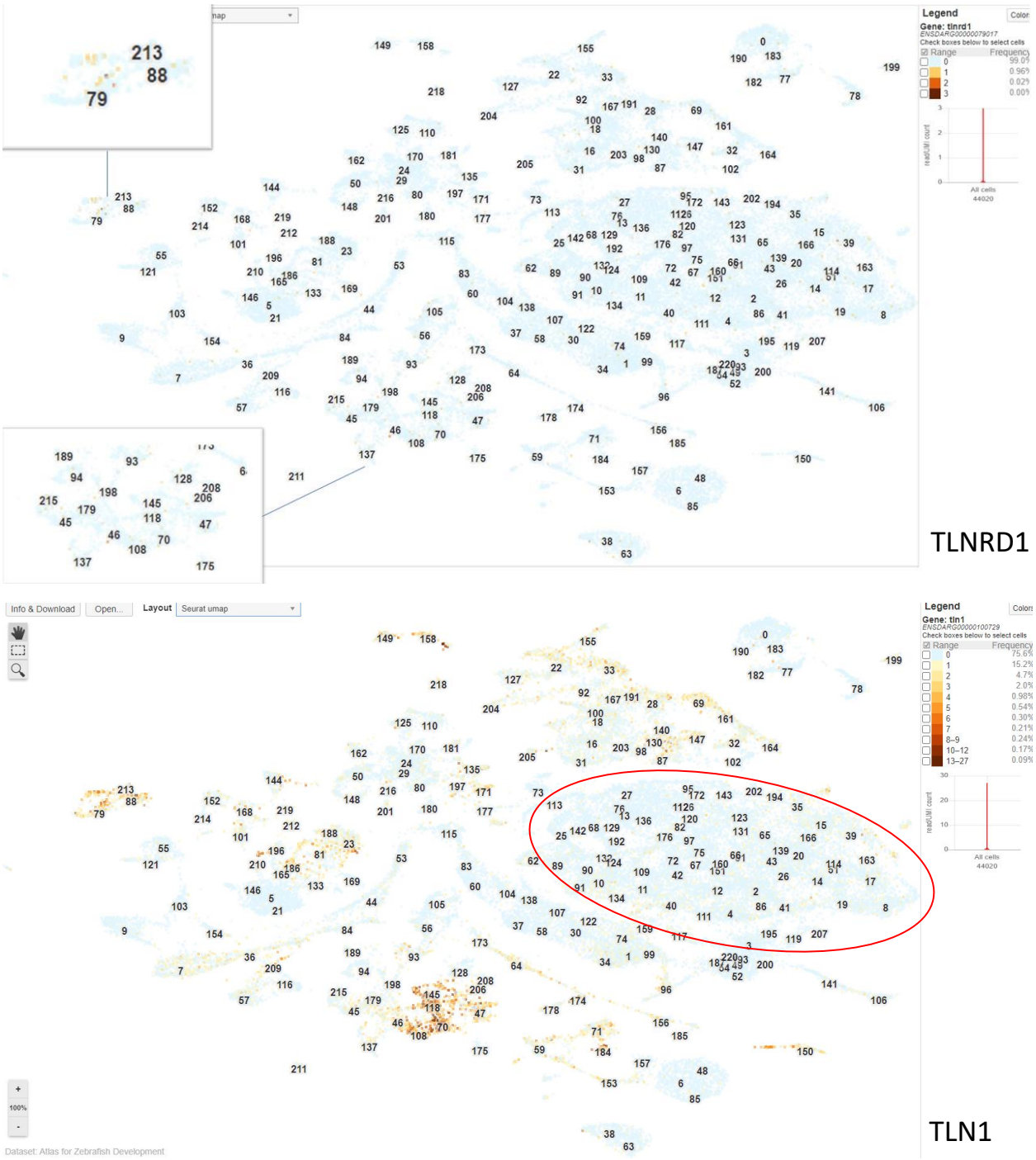

Figure 6. RNA expression patterns of TLNRD1 (top) and TLN1 (bottom). This figure visualizes how much the different cells and tissues of a zebrafish embryo express the respective genes. As shown, TLNRD1 is rather poorly expressed within the database, and the regions with the highest grades of expression are separated in boxes. In comparison TLN1 is a far more commonly expressed gene, with more variation of expression levels and tissues of expression. The area of mainly neural tissues in the dashed oval region is marked in the lower picture with a red circle. (Farnsworth et al. 2020)

2.5 Microinjections with sgRNA and CRISPR-CAS9

After finishing the analysis of the naturally spawned embryo group, another way of obtaining information about the role of TLNRD1 was planned and carried out. Because the previous embryo sample group did not showcase statistically significant results, microinjection assay was performed.

In order to observe how the *tlnrd1*-gene is functioning, a set of microinjections were conducted to recently fertilized embryos. The injection mixture contained a solution of sgRNAs, Cas9 enzyme, KCl and H_2O. The point of injecting the embryos with sgRNAs was to observe if genetic modification of *tlnrd1* with sgRNAs, produces visible phenotypes and malformations in the vasculature of developing zebrafish embryos. The assay was done with using two different sgRNA sample groups and one un-injected control group.

After the injections, the embryos were cultured and screened daily similarly to the previous embryo group. They were also imaged, cells were lysed and DNA extraction was conducted again. The image data of the microinjected embryos was analysed and collected for visualisation. First the imaging data was compared visually between the groups (Figure 7) and the larger and more severe deformations were highlighted (Figure 8). The differences in vasculature were further pinpointed in comparative images (Figure 9).

Figure 7. – Microinjected sample groups and visual differences presented. As seen the negative control samples are presenting a more normal vasculature structure than the control sgRNA or the tlnrd1-sgRNA groups. The anatomical changes of the fish are more visible in the microinjected sample group as seen from lower right from the tlnrd1-sgRNA group.

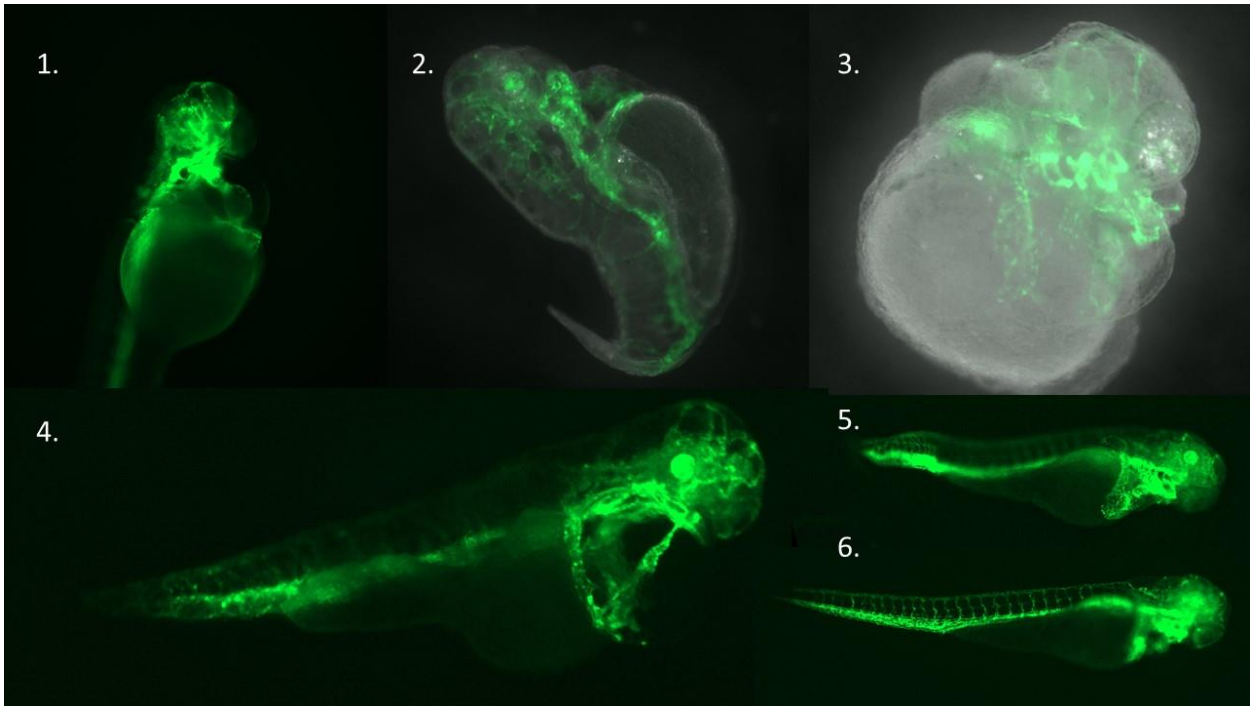

Figure 8. – Notable anatomical and vasculature deformations among the microinjected samples. 1. Excess space around the pericardium 2. Deformed body and vasculature, 3. A seriously deformed embryo with only a partially developed head and vasculature, 4. Deformed heart with even greater empty space around the pericardium, 5. Curved spine and irregular vasculature and 6. An upwards curving tail. Although these visible deformations look significant, due to the quality of the images and lack of ability to measure the vasculature parameters, some were excluded from the statistical data. (Samples like 2. 3. and 4.)

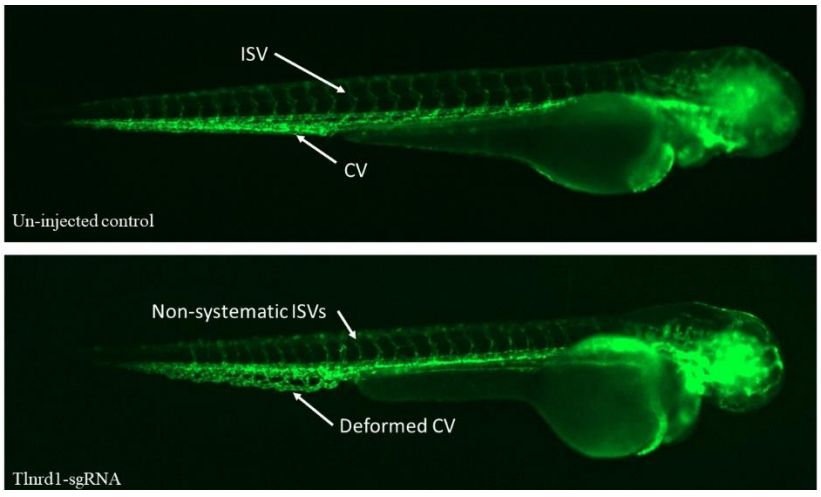

Figure 9. – The differences of the not injected negative control embryos (top) and the microinjected tlnrd1-sgRNA embryos (bottom). The caudal vein (CV) of the tlnrd1 group is more deformed and branching than in the negative control. Also, a slight disarray and loss of integrity is seen in the dorsal intersegmental veins (ISV).

2.6 Physical parameters of the vasculature (microinjections)

Like prior with section 2.3, the same physical parameters were measured among the fluorescent image data. The measurement for embryo body length, CV width and ISV widths were done similarly for the microinjected samples. The values were charted and visualised and the statistical differences and significance were measured. This was conducted to find out if the microinjections significantly altered the vasculature of the embryos. Comparative parameter data was visualised (Figure 10) and the statistical significance was verified with one-way ANOVA (Table 4.) and Dunnett's Post Hoc tests (Table 5).

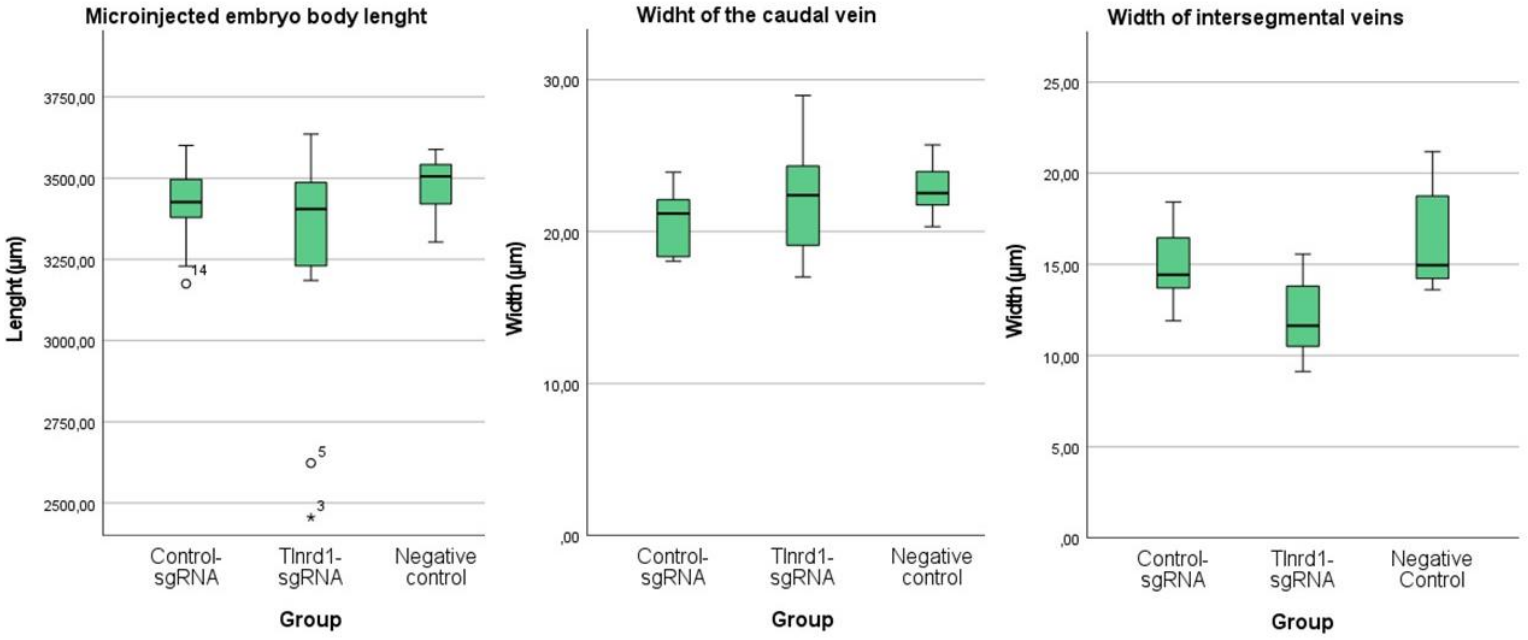

Figure 10. The parameter data from microinjected embryos showcased as a boxplot. The measured parameters are the same that were introduced in Figure 6. In total the sample numbers in microinjected embryos were 33 from which 29 were successfully measured, due to the positive inheritance of the eGFP fluorescent marker. In the statistical data the groups were marked as follows: not injected negative control = 0, control-sgRNA = 1, tlnrd1-sgRNA = 2.

Table 4. - One-way ANOVA test for microinjected sample groups

		Sum of Squares	df	Mean Square	F	Sig.
Body length	Between Groups	207834,478	2	103917,239	1,777	0,186
	Within Groups	1754151,179	30	58471,706		
	Total	1961985,657	32			
IS vein width	Between Groups	95,316	2	47,658	8,881	**0,001***
	Within Groups	139,526	26	5,366		
	Total	234,842	28			
Caudal vein width	Between Groups	22,733	2	11,367	1,365	0,273
	Within Groups	216,582	26	8,330		
	Total	239,315	28			

Table 5. Dunnett's Post Hoc test between microinjected sample groups

Dependent Variable		(I) group	(J) group	Mean Difference (I-J)	Std. Error	Sig.	95% Confidence Interval	
							Lower Bound	Upper Bound
Body length	Dunnett t (2-sided)[a]	0	2	195,27354	113,3619	0,170	-68,9048	459,4519
		1	2	134,36015	94,84539	0,288	-86,6673	355,3876
IS vein width	Dunnett t (2-sided)[a]	0	2	4,42887*	1,10174	**<0,001**	1,8407	7,0170
		1	2	2,77724*	0,99189	**0,018**	0,4471	5,1073
Caudal vein width	Dunnett t (2-sided)[a]	0	2	0,47240	1,37266	0,921	-2,7522	3,6970
		1	2	-1,64783	1,23579	0,330	-4,5509	1,2552

*. The mean difference is significant at the 0.05 level.

a. Dunnett t-tests treat one group as a control, and compare all other groups against it.

2.7 T7 endonuclease assay

Because of the genetic edition of the target gene *tlnrd1*, done with CRISPR-Cas9, the regular form of PCR can't be used to determine the "genotype" of these embryos. Instead a T7 endonuclease assay was performed, to highlight the amount of genetic edition, within the embryos.

In the assay, the endonuclease cleaves all forms of mismatched dsDNA, resulting in multiple bands, from which the genetic alteration and fraction of gene edition can be calculated. This was performed in order to connect the data from the fluorescent image data set and the genetic data set.

The assay was conducted according to (Guschin *et al.* 2010), and the visualisation was done with the aid of a agarose gel electrophoresis. (Figure 11.)

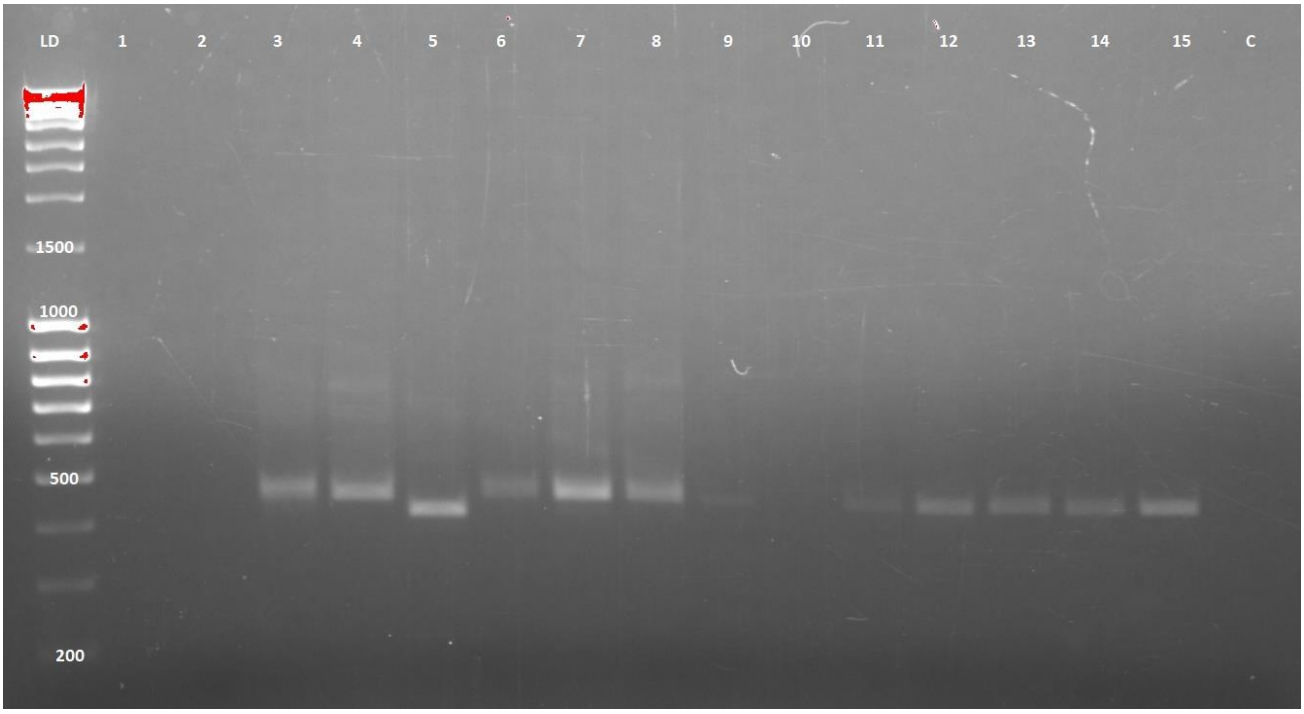

Figure 11. T7 endonuclease assay results. Samples 1-15 are all from the tlnrd1-sgRNA injected embryos treated with the T7 endonuclease enzyme, and C is a negative water control. The ladder used was MassRuler DNA Ladder Mix and the gel was 2% agarose gel run in 100V for 1 hours.

3 Discussion

All together the results can be divided into three major categories. Genetic results (genotyping, gene sequence and the RNA expression database), visible phenotype and vascular integrity results (image comparison and analysis) and statistical analysis of measured physical parameters of veins.

3.1 Genetic data

Table 1. shows the occurrence of the different genotypes within the naturally spawn embryo group, and based on the numbers, it was assumed that the genetic inheritance is most likely following the Mendelian inheritance pattern (distribution approx. 25% per each genotype). This was confirmed by performing a Hardy-Weinberg chi-square test (Table 2.), which was compared to the expected distribution of the mendelian inheritance. And since the P-value exceeds 0,01 ($p = 0,866$) this means no significant difference between the two distributions, meaning the genetic distribution of the naturally spawn sample group complies with the mendelian inheritance values.

The method of PCR used for genotyping the TLNRD1 knockout embryos, was relatively standard, but the two-phase operation made it quite resource consuming to genotype larger sample groups than approx. 60 embryos. During the experimental part, multiple times the genotyping failed for unclear reasons, resulting in partially empty agarose gels. The genotyping was continued repetitively until the current sample size was reached. The main speculations of failure were errors in lysing the embryonal DNA, pipetting errors or the low concentrations of template DNA. Some editions of the PCR protocols could have affected the genotyping (changing the annealing temperatures of the different PCR programs.). Initially there were more than 59 embryos to do genotyping on, but upon inspecting the visual phenotypes, it was concluded that there is no use to genotype embryos further, due to the lack of clear and visible phenotypes or notable changes in the vasculature structures.

The genetic sequence data obtained from Eurofins Scientific was done for one WT and one M samples, which were supposed to have the length of 445 bp, according to the PCR protocol. Among the sequenced samples, the aligned results show a moderate insertion of 78 bp in-frame sequence in the TLNRD1 mutant sample, presented in Figure 5. When the M-sample was aligned and compared to the wild type, a total of eight singular point mutations was observed. The effect of

the insertion is unclear, since in the microscopy images there is no that significant differences between the mutant and wild type embryos, neither in their general anatomy or between their vascular structures. In addition, the sequencing was done just for a total of 4 samples (2 M and 2 WT) and in few obtained results, the sequences were too short to be correspond to the tlnrd1 sequence, as a result of incomplete polymerisation or poor PCR yield.

3.2 Cell browser data

As seen from Figure 6. when comparing the RNA expression patterns and levels between *tlnrd1* and *tln1* genes from the established database (Farnsworth *et al.* 2020), *tlnrd1* shows a much lower rate of expression than *tln1*. The tissues where our target gene is most visibly expressed (most visible coloured spots in range of 1-3), is the epithelial area of blood vessels (cluster 79) and mesodermal areas of blood vessels (clusters 88 and 213). As seen with other spots (any coloured spot above range 1), the distribution of tissues and cells where *tlnrd1* is expressed, are quite scattered around all of the clusters. Noticeably the few sites of relatively active tissues include the pharyngeal endotherm (cluster 46), mesodermal HSCs (cluster 38) and the ectodermal neuroblasts of the spinal cord (cluster 39).

In comparison, *tln1* is a far wider expressed gene, and the range of expression is far wider than the expression range of *tlnrd1* (*tlnrd1* has a range of 1 to 3 vs. *tln1* has the range of 1 to 27). The tissues where *tln1* is mostly expressed include the same tissues as *tlnrd1*, but in addition to these tissues, significant expression (coloured spots above range 6) are visible in the ectodermal integument basal cells (clusters 23, 47, 70, 118), ectodermal basal cells of the fins (clusters 108 and 145), mesodermal leucocyte neutrophils (cluster 150), mesodermal cephalic muscle cells (cluster 154), the mesodermal notochord (cluster 158), mesodermal myeloid lineage macrophages (cluster 184) and mesodermal spleen epithelial cells (cluster 210). In addition to these tissues and cell types, *tln1* is present in many of the clusters visible in the database. What is however common for both genes, is that they are not strongly expressed in the dashed oval region (red circle) which is mostly composed from the clusters that are related to neurons and the CNS. This indicates that these two genes are not as strongly related to the functions and development of neural tissues as they are in epithelial tissues.

3.3 Vascular integrity and phenotypes

In Figure 2. the first sings of visual phenotypes for the naturally spawned embryos can be seen. Each genotype at first glance shares overall quite similar vasculature structure and single differences between the embryos are quite limited. Most of the embryos have relatively normal vasculatures and they lack any specific kinds of morphological malformations, as seen later when comparing the data among the sgRNA microinjected samples. One single noteworthy feature was observed from the sample group, which was the deformed “hunched back” which was present in total of 7/59 samples. Although this seems intriguing, all of the genotyped samples had at least one embryo with the hunched back, so it is not considered to be a significant finding, that would be relevant in the vascular anatomy or integrity of these embryos.

To confirm whether the different genotypes have an effect on the vasculature of these embryos, three physical parameters were measured among the samples. The overall body length of the embryos, and the widths of both the posterior caudal vein (averages from 3 measuring points) and the dorsal inter segmental veins (averages of 5 measuring points) which are among the structures that develop via branching angiogenesis as established in the introduction.

As seen from figure 4. the box plots are more or less close to the same line, and the histograms align relatively similarly to the normal distribution curve. To confirm the statistical significance between the genotype and the measured parameters, one-way ANOVA test was performed, results visualised in Table 3. As seen from the Sig. column, none of the obtained P-values were significant ($P \leq 0{,}05$), which indicates that there is no clear link between the physical parameters and the different genotype.

The total sample size for these embryos and measured parameters was in the end N = 46, since 13 of the genotyped samples lacked the mCherry fluorescent marker, thus measuring the vessel structures was impossible. The body length measurement was unaffected by this, since the overall body of the fish was still visible, although the vasculature was not. It could be possible that a larger sample size would present more significant results.

3.4 Vascular integrity and phenotypes (microinjection)

Upon inspecting Figure 7, the sample groups of sgRNA-injected embryos, the vascular differences are more apparent and visibly noticeable. When compared with the un-injected control, it is seen that both the control-sgRNA and tlnrd1 groups have changes in their vasculature, especially in the areas of interest, the caudal vein (CV) and the inter segmental veins (ISV). These differences are highlighted more in Figure 9. Mainly the integrity of the CV is less systematic and in some samples the vein is crooked and there seems to be some forms of separate vascular pillars and off branching veins similarly to branching angiogenesis or intussusceptive vascular remodelling. The morphological differences of the ISVs are less visible but as highlighted in Fig. 9, the sample presented shows that some of the ISVs are placed irregularly compared to the clear dorsal patters of the negative control samples. In addition, the showcased ISVs affected by the sgRNA injections are more morphologically deformed and crooked than the un-injected control ISVs.

Figure 8. showcases some of the most extreme documented deformations in both the general anatomy and the vasculature among the injected embryos. Samples 2 and 3 have clearly interrupted development at some earlier stage, while sample 2 has developed a tail of some shorts, embryo 3 does not have any other development beside the head, eyes, the yolk sac. However, both of these severely malformed embryos showcase the expression of eGFP, meaning vascular development was still present at some degrees.

Samples 1 and 4 are more developed but they noticeably have deformed vasculature around their heart. In sample 1 the area surrounding the pericardium is much larger than in the negative control embryos. In sample 4, the heart is severely deformed to a thin myocardial fibre, with a large excess space around the pericardium. And among the examined embryos sample 4 is one of the most outstanding, since the vascular deformations are present also in many other areas, such as the dorsal ISVs and the posterior CV and dorsal aorta. However, the scale of deformations present in the entire system of the embryo are probably not singularly linked to the sgRNA-injection. For the recently fertilized embryo, the injection is a rough process, and nearly half of the injected embryos die during the culturing process. And one singular deformed embryo, surviving to the stage of imaging, is probably too little proof of the significance of TLNRD1 in vascular development, since as previously established multiple other proteins and cells partake in angiogenetic development.

Samples 5 and 6 are the embryos in Figure 8 closest to normally developed vasculature. Slight disarray can be seen in their ISV region, but the bigger malformations in these samples are the anatomical structures. Sample 5 is rather small in body size with a clearly curved spine. Sample 6 on the other hand has an upward curved tail and slightly altered ISVs.

In Figure 10. The boxplots for the microinjected samples are shown. Compared to the naturally spawn embryo group, slightly more variation is visible in the positions of the plots. Especially in the graph showcasing ISV widths. Tables 4 and 5 show the statistical analysis for the physical parameters measured from the vasculature. The used tests are One-way ANOVA and the Dunnett's Post Hoc test between the groups. Here we notice that the width of ISVs is the only parameter that showcases statistical significance, with a ($P = 0{,}001$). The significance is also confirmed with the Dunnett's Post Hoc test, to calculate the rate of significance between the groups, and the results show that between the negative control and the tlnrd1 group the significance is great ($P < 0{,}001$) and between the tlnrd1 and control-sgRNA groups the significance is $P = 0{,}018$, which is still considered to be significant. None of the other parameters however display statistical significance among the microinjected samples.

3.5 T7 endonuclease assay data

The last piece of data is in Figure 11. The agarose gel from the T7 endonuclease assay. However, as seen from this gel, the T7 endonuclease assay lacks any separate bands. Upon analysing the image of the gel, with inverted colours, the samples would shown contrast spikes, upon measuring them with ImageJ's Fiji software. This did not happen, so the lack of clear bands in the T7 gel indicates that the microinjected samples lack any mismatched DNA. And this means then, that either the Crispr-Cas9 injection did not work as intended or the T7 endonuclease assay failed. Although in band number 5 it is seen, that it does not align with the other samples, indicating something happened to that sample, and the PCR product was indeed shorter than the other samples, obtained from the injected embryos. It could have been possible to cut the band and send it for sequencing to confirm this, but we did not think it was necessary overall, since the T7 assay did not provide positive results.

4 Conclusion

What can we conclude based on our data? At first it could be argued that the vast amount of insignificant statistics and lack of noticeable phenotypical changes would indicate that the mutations within *tlnrd1* do not showcase huge alterations in the vasculature system and vein integrity. Within the microinjected samples of tlnrd1 showcasing statistical significance in the widths of the ISVs, it could be argued that the gene could play into this difference. It has been already hinted by Tatarano *et al.* that the miRNA binding to specific genes may decrease cell proliferation and other functions, so it could be debated that the microinjected sgRNA samples for TLNRD1 had a similar effect, but on the entire vasculature. As pointed out in Figure 9, the tlnrd1 injected samples have more visible vascular deformations and lack of vessel integrity than the negative controls and partially the control-sgRNA samples. Although this is not similarly seen in naturally recombined embryos.

However, the RNA expression patterns of TLNRD1 point out how little the expression of *tlnrd1* is compared to the homologue protein talin, which has a much distinguished and better-established role related to cell proliferation, angiogenesis and adhesion. Plus, the sheer size of TLNRD1 is just rising gestions, is such a small protein really as significant in angiogenesis as previously thought?

To achieve a certain and exact conclusion based on these results, it is quite difficult to pinpoint one singular fact. The sgRNA effected embryos do showcase alterations in vasculature, but the significance is seen only in the ISV region and parameters. Other parameters measured do not showcase statistical difference, not in the naturally spawn embryos or in the microinjections regarding to body length and CV widths. The mutant *tlnrd1*-zebrafish line develops seemingly normally in the naturally spawn embryos, and the microinjected embryos showcase malformations due to effects of CRISPR-Cas9 and the sgRNAs.

Since the embryos were only *tlnrd1* mutants, it could be possible regular *tln1* functioned without issues, and thus the seen vascular development in the naturally spawn fish line did not include huge deformations. It would be intriguing to see what would happen, if the *tln1* gene is knocked out, and the *tlnrd1* gene still being functional and how this would be affecting on the vasculature development. Since multiple different growth factors take part in angiogenesis, it is a possibility that the vascular development is mediated with alternative pathways, if one is blocked or deleted.

What comes to drugs and targeting angiogenesis, it might be that TLNRD1 is not the most prominent target for antiangiogenic drug, based on the reasons listed earlier. Although angiogenesis is affecting multiple diseases like malignant cancers, ischemia, inflammatory conditions, infections and immune disorders, the primary developed drugs are related to anti-inflammatory and growth factor inhibitors than direct cell adhesion blockers. (Teleanu *et al.* 2019)

The most prominent drugs for angiogenesis, are used to tackle various cancers. According to the report of National Institute of Health's Cancer Institute, the FDA has approved altogether 14 antiangiogenic drugs by 2018 in the USA. (NIH 2018) Out of these drugs 11 are small molecule receptor tyrosine kinase inhibitors, two are monoclonal antibodies acting as VEGF and VEGFR2 inhibitors and one drug (Ziv-Aflibercept) is a recombinant protein drug, which acts as a decoy receptor for extracellular VEGF. (Drugbank 2022)

The topic and exact function of TLNRD1 remains still unrevealed, but as discussed in this thesis, the protein seems to effect slightly vascular development, and more research on the topic would be needed.

5 Materials and methods

Multiple different types of methods were used during this project, mainly consisting of molecular biology methods (PCR, electrophoresis, oligonuclease-7 assay and CRISPR-Cas9) and different imaging and microscopy techniques and statistical analyses. Other methods include online database searches, zebrafish handling and embryo culturing. In this section, more detailed information is provided.

5.1 Embryo production

The first step of the project was the mating of zebrafish (*Danio rerio*) and embryo collecting. This was repeated each time prior creating a new group of samples. Maximum of 5 male and 5 female fish were selected in the specific mating tank. The fish lines used in this experiment were a either LS109 (TLNRD1 knockout line *tlnrd1*^{tcb2} with a mCherry fluorescent marker), LS111 or LS112 (*kdrl* line with eGFP marker with unedited gene of *tlnrd1*). The tanks were left in 26°C overnight and the next morning the eggs were harvested. Upon inspection of the recently fertilized eggs, they were screened and separated from unfertilized ones and placed on a petri dish maximum 50 eggs on each. The embryos were cultured in 28,5°C incubator in E3-medium (34.8 g NaCl, 1.6 g KCl,

5.8 g $CaCl_2 \cdot 2\ H_2O$ and 9.78 g $MgCl_2 \cdot 6H_2O$ filled up with 2 l of Milli Q-H_2O) with added 1-phenyl 2-thiourea (PTU, Sigma-Aldrich P7629) to inhibit cellular melanin production. The embryos were cultured for 3-4 days and each day the plates were screened for sorting out unfertilized or contaminated eggs. After the first overnight incubation, additional pronase (10 mg/ml, Roche Cat. No. 10 165 921 001) solution was added to fasten embryo hatching.

The procedure for obtaining embryos for microinjections specifically, was done quite similarly, except upon placing fish in the mating tank the females and males were separated by a wall for overnight, which was removed on the following morning, to control the mating time and harvest the eggs before their first cell division.

5.2 Microinjections

Table 6. – The sequences of the used sgRNAs in the microinjection assay

sgRNA	Sequence
Control -sgRNA (Slc45a2-1)	TTCTAATACGACTCACTATAGGTTTGGGAACCGGTCT GATGTTTTAGAGCTAGA
Control -sgRNA (Slc45a2-2)	TTCTAATACGACTCACTATAGTTCTCATCGGGATAAA GAGGTTTTAGAGCTAGA
TLNRD1-sgRNA9	TTCTAATACGACTCACTATAGCTCGGGGAAATCAGAT AGCGGTTTTAGAGCTAGA
TLNRD1-sgRNA14	TTCTAATACGACTCACTATAGTTAGCGGCAGCTTGCA ACAAGTTTTAGAGCTAGA
TLNRD1-sgRNA24	TTCTAATACGACTCACTATAGCTATGGCTAGTAGTGG CTCGGTTTTAGAGCTAGA
TLNRD1-sgRNA25	TTCTAATACGACTCACTATAGCACACTACTATGGCTA GTAGGTTTTAGAGCTAGA

Microinjections were used to edit the genome of the fertilized eggs with the aid of single guide RNA's and CRISPR-Cas9 targeting the TLNRD1 gene. The general protocol of performing the injections was done by following a publication by Hoshijama (*et al.* 2019), with slight alterations with the different buffers and reagents. Within 1 hour after egg harvesting, the eggs were collected on an injection plate, where they were injected with a 2,3 nl of sample solution, using Nanoject II Auto-Nanoliter Injector (by Drummond scientific company). The injection solutions consisted from different volumes of sgRNAs, CAS9-enzyme (EnGen™ Spy Cas9 NLS NEB #M0646), KCl and H_2O. The process was repeated for two sample groups, control-sgRNA (mixture of two

Slc45a2-sgRNAs 1 and 2) and TLNRD1-sgRNA (mixture of different sg-RNAs 9, 14, 24 and 25). Sequences of the used RNAs are presented in Table 6.

These two groups were compared to the un-injected embryo group (negative control). After injecting all the eggs, they were put on a petri dish with E3-PTU medium and 100 µl of Penicillin-Streptomycin mixture (ThermoFisher Scientific 15140122). After the injections, the plates were incubated at 28,5°C for 3 days, similarly screening and removing the unfertilized and contaminated eggs, changing the medium and counting each day how many embryos survived the injection and how many of them developed further.

5.3 Imaging

The following step of the project was to image the embryos and their vasculature system. Prior imaging the embryos (max. 5 days old) were anesthetized using tricaine methane sulfonate MS222 with 167mg/l on the plate (Sigma-Aldrich E10521-50G). Then a separate smaller imaging petri dish was made filling it with E3 medium and MS222. The imaging device used was the fluorescence microscope Zeiss AxioZoom.V16.

The embryos were placed one at the time to the imagining plate carefully with a pipette and full body images were taken from them using two to three channels, bright field, GFP or TEX-R, depending on the used fish line and their fluorescent marker. The images were taken with the Hamamatsu camera, using 32x – 40x zoom and 3.8 µm resolution. The focus of the images was on the blood vessels in the posterior and dorsal sides of the embryo. Also, the overall anatomy of the embryo was inspected during imaging.

Upon completing the imaging for each embryo, they were placed carefully in an Eppendorf tube labelled correctly one at the time and the excess liquid was removed with a pipette. After this the samples were frozen in - 20°C for further analysis.

5.4 Genotyping

Table 7. – The sequences of the used primers in the genotyping assay

Primer	Sequence		
Tlnrd1_L3	TCATTTACATGGCACGAAGAAC	Tlnrd1_R4	GGTGAGGTTCTTCAGGATGTTC
Tlnrd1_R3	ATAGACAGCTCCTTGGTTCTGG	Tlnrd1_L4	CGAGTGAAGTTTCATGTTTTCG

Genotyping a sample group was done with PCR and agarose gel electrophoresis. The samples were prepared for PCR using a single embryo DNA extraction protocol Hotshot method (Meeker *et al.* 2007) Carrying out the genotyping PCR for the project needed two consecutive PCR reactions, with two sets of different primers (Sequences can be found in Table 7). The first reaction is targeting a 1165 bp sequence with the primers marked L3 and R4 (annealing temperature 67,1°C), and the second approx. 445 bp sequence with the primers L4 and R3 (annealing temperature 66,8°C). The reaction mix was composed of RNA free water, Phusion Hot Start II DNA Polymerase (2 U/µL Thermofischer F549S) buffer and enzyme, primers, dNTP-mixture and the template DNA. In the first reaction the template DNA was extracted from the embryo samples and the first reaction PCR product was used as a template for the second reaction. Both reactions were run for 30 cycles.

For visualizing the genotype differences, the second PCR product was run on agarose gel electrophoresis (Sigma-Aldrich A4718-100G), using a 2% gel made in 100 ml of 1x Tris Acetate-EDTA buffer (TAE, Sigma-Aldrich T6025). Midori Green DNA dye 5µl (Fisher Scientific NC0434746) was added to the gel before pouring it in the gel mould. For electrophoresis GeneRuler DNA Ladder Mix 6x (Thermofischer Scientific SM0331) was used and the samples were mixed with the DNA Gel Loading Due 6x (Thermofischer Scientific R0611). Depending on the sample group the wells were loaded with 10 to 20 µl of PCR product. The gel was run using 100 V for 1 hour. The ready gel was then imaged with the Biorad Gel Doc XR+ Gel Documentation System.

5.5 Genetic sequencing

After the gel electrophoresis some bands were selected for sequencing analysis, which was done by using the commercial services provided by Eurofins Scientific. The selected DNA bands were cut from the gel under a UV-light and then purified and prepared with a Macherey-Nagel™ NucleoSpin Gel and PCR Clean-Up Kit (Macherey-Nagel™ 740609.50). The sequencing samples were mixed with their respective primers in barcode labelled Eppendorf tubes, which were sent to Eurofins Scientific. After sequencing the data was sent from Eurofins Scientific online and the sequences were analysed with computational BLAST and alignment tools. The obtained sequences were compared with known sequences of the TLNRD1 gene.

5.6 T7 endonuclease assay

When considering the microinjections and the CRISPR gene edition, T7 endonuclease assay was used as a tool before the agarose gel electrophoresis, to observe the concrete effects of the genetic modifications. The PCR product was purified using the Macherey-Nagel™ NucleoSpin Gel and PCR Clean-Up Kit (Macherey-Nagel™ 740609.50), after which the T7 endonuclease assay (EnGen® sgRNA Synthesis Kit, S. pyogenes, E3322S) was performed to the samples. The samples were hybridized first before adding the T7 Endonuclease I enzyme to the samples, then incubation for 15 minutes at 37 °C and after that the reaction was stopped with adding EDTA to the samples. Then a similar agarose gel electrophoresis was run with same protocol as in the genotyping and the gel was imaged. In the end the gene edition was analysed by using ImageJ's Fiji-image processing package. The analysis focused on contrast measurement tools and using the obtained values to a given equation. The point of conducting this assay was to measure how much the Crispr-Cas9 affected the edition of the *tlnrd1*-gene. The T7 endonuclease assay is used for cutting any mismatch from the dsDNA.

The fragmented PCR products should show in the gel with multiple bands, from which the fraction of cleavage should be calculated using the following equation provided by (Guschin *et al.* 2010).

$$Presentage\ of\ gene\ modification = 100 \times (1 - (1 - fraction\ cleaved)^{\frac{1}{2}})$$

When comparing the contrast spikes between the bands on the gel, we could establish the percentage of gene editions for each sample. (Guschin *et al.* 2010)

5.7 Database search

Online database search was also performed as a part of the project by using the Single cell transcriptome atlas for zebrafish embryo development (Farnsworth *et.al* 2020). The data was obtained from the UCSC Cell Browser library. This section was done to find out information of the TLNRD1 gene and in which tissues and in what quantities the gene is expressed. As a comparison value, the expression of talin encoding gene TLN1 was also observed from the database.

5.8 Image analysis

Upon image analysis, the bands of the gels were counted and documented in a table, showing in which ratios the genotypes were occurring in the sample group. Also, analysing and editing the full body microscopy photos of the embryos was a part of image analysis. During this, several parameters were measured from the photos, such as cardinal vein widths, dorsal aorta width and body length of the embryos. The measurements were done with Fiji and documented with IBM SPSS software for statistical analysis.

5.9 Statistics

And finally, statistical analysis and data visualization was performed using IMB SPSS 28 Statistics software. For the successfully genotyped embryos, the Hardy-Weinberg chi-square test was done to confirm the inheritance pattern of the *tlnrd1*-gene against traditional Mendelian distribution. The frequencies of the measured blood vessel parameters among the normally spawned embryos are showcased in a histogram, and the differences between parameters and sample groups are shown as boxplots. The statistical tests between the variable groups are Dunnett's post-hoc and one-way ANOVA tests. The P-values between the groups were obtained and shown in charts where the statistical significance was highlighted, whenever the result was significant.

6 Ethical and confidentiality considerations

As this thesis included working with an animal model (*Danio rerio*) ethical considerations were included to the thesis, and the respective project plan. In this study, we used only newly spawned zebrafish embryos, which were always less than 5 days old. According to the legislation, these embryos are not considered as animals yet, and therefore separate license or a project plan for animal testing is not necessary. However, adult zebrafish were used to spawn new embryos, which in this case, were generated and kept under the licenses ESAVI/9339/04.10.07/2016, ESAVI/37571/2019 and ESAVI/31414/2020 (National Animal Experimentation Board, Regional State Administrative Agency for Southern Finland). The adult fish were taken care according to the regulations and rules of the Central Animal Laboratory of the University of Turku by respectively trained professional personnel. The conductor of this project has also completed animal model specific training for handling zebrafish adults (when producing embryos) prior of making this study and the respective document of proof about the training was submitted for the supervisor of this project.

The only procedure which could be interpreted as "invasive" for the embryos, was the microinjection, but as stated prior, since the experiments are always done with under 5-day old fish embryos, this was not a major concern.

Due the nature of this study of being a Master's Thesis project in the field of basic research, there are no confidentiality issues regarding this study, neither does it have any commercial availability.

7 Acknowledgements

First of all, I would like to thank my supervisor Ilkka Paatero of the continuous and professional support he has provided me during this entire process. He has been patient and encouraging despite all of the unexpected difficulties in the project and has aided me to learn important skills in academic research. Another round of thanks would be designated towards Professor Johanna Ivaska from the University of Turku and Guillaume Jacquemet from Åbo Akademi University, for being the collaborators in my thesis project. I would like to thank also all the other colleagues working in the Zebrafish core, and the laboratory scientists Petra Laasola and Jenni Siivonen of the Ivaska group, for aiding me to work around the laboratory during the experimental part of the thesis. I would also thank the animal caretakers and personnel of Central Animal Laboratory of the University of Turku for taking care of the zebrafish and keeping up their good living conditions.

Completing this project and the degree has not been an easy task so last but not least, I would say my sincerest thanks for all the people who have supported me during this time, friends, family and the personnel of the faculty. Thank you.

8 Abbreviations

TLNRD1 - Talin rod domain-containing protein 1

tlnrd1 – Talin rod domain-containing protein 1 gene

eGFP – enhanced Green fluorescent protein

mCherry – monomeric Red fluorescent protein

EPC – Endothelial progenitor cell

EC – Endothelial cell

HSC – Hematopoietic stem cell

ECM – Extra cellular matrix

MSC – Mesenchymal stem cell

FGF – Fibroblast growth factor

VEGF – Vascular endothelial growth factor

RIAM – Rap1-GTP–interacting adaptor molecule

kdrl – kinase insert domain receptor like

ZO-1 – Zonula occludens-1 aka. Tight junction protein 1

PDGF – Platelet derived growth factor

MMP – Matrix metalloproteinase

TGFβ – Transforming growth factor beta

HIF-1 – Hypoxia inducible factor 1

ANG – Angiopoietin

TIE – Tyrosine kinase with immunoglobulin and EGF like domain

KANK - Kidney Ankyrin Repeat-Containing Protein

References

Abu-Ghazaleh, R., Kabir, J., Jia, H., Lobo, M., & Zachary, I. (2001). Src mediates stimulation by vascular endothelial growth factor of the phosphorylation of focal adhesion kinase at tyrosine 861, and migration and anti-apoptosis in endothelial cells. The Biochemical journal, 360(Pt 1), 255–264. https://doi.org/10.1042/0264-6021:3600255

Adair TH, Montani JP. Angiogenesis. San Rafael (CA): Morgan & Claypool Life Sciences; 2010. Chapter 1, Overview of Angiogenesis. Available from: https://www.ncbi.nlm.nih.gov/books/NBK53238/

Alvero, A. B., Fu, H. H., Holmberg, J., Visintin, I., Mor, L., Marquina, C. C., Oidtman, J., Silasi, D. A., & Mor, G. (2009). Stem-like ovarian cancer cells can serve as tumor vascular progenitors. Stem cells (Dayton, Ohio), 27(10), 2405–2413. https://doi.org/10.1002/stem.191

Asahara, T., Murohara, T., Sullivan, A., Silver, M., van der Zee, R., Li, T., Witzenbichler, B., Schatteman, G., & Isner, J. M. (1997). Isolation of putative progenitor endothelial cells for angiogenesis. Science (New York, N.Y.), 275(5302), 964–967. https://doi.org/10.1126/science.275.5302.964

Ayala-Domínguez, L., Olmedo-Nieva, L., Muñoz-Bello, J. O., Contreras-Paredes, A., Manzo-Merino, J., Martínez-Ramírez, I., & Lizano, M. (2019). Mechanisms of Vasculogenic Mimicry in Ovarian Cancer. Frontiers in oncology, 9, 998. https://doi.org/10.3389/fonc.2019.00998

Baba, Y., Nosho, K., Shima, K., Irahara, N., Chan, A. T., Meyerhardt, J. A., Chung, D. C., Giovannucci, E. L., Fuchs, C. S., & Ogino, S. (2010). HIF1A overexpression is associated with poor prognosis in a cohort of 731 colorectal cancers. The American journal of pathology, 176(5), 2292–2301. https://doi.org/10.2353/ajpath.2010.090972

Bárdos, J. I., & Ashcroft, M. (2005). Negative and positive regulation of HIF-1: a complex network. Biochimica et biophysica acta, 1755(2), 107–120. https://doi.org/10.1016/j.bbcan.2005.05.001

Barleon, B., Reusch, P., Totzke, F., Herzog, C., Keck, C., Martiny-Baron, G., & Marmé, D. (2001). Soluble VEGFR-1 secreted by endothelial cells and monocytes is present in human serum and plasma from healthy donors. Angiogenesis, 4(2), 143–154. https://doi.org/10.1023/a:1012245307884

Basile, J. R., Barac, A., Zhu, T., Guan, K. L., & Gutkind, J. S. (2004). Class IV semaphorins promote angiogenesis by stimulating Rho-initiated pathways through plexin-B. Cancer research, 64(15), 5212–5224. https://doi.org/10.1158/0008-5472.CAN-04-0126

Bate, N., Gingras, A. R., Bachir, A., Horwitz, R., Ye, F., Patel, B., Goult, B. T., & Critchley, D. R. (2012). Talin contains a C-terminal calpain2 cleavage site important in focal adhesion dynamics. PloS one, 7(4), e34461. https://doi.org/10.1371/journal.pone.0034461

Bellik, L., Vinci, M. C., Filippi, S., Ledda, F., & Parenti, A. (2005). Intracellular pathways triggered by the selective FLT-1-agonist placental growth factor in vascular smooth muscle cells exposed to hypoxia. British journal of pharmacology, 146(4), 568–575. https://doi.org/10.1038/sj.bjp.0706347

Bedell, V. M., Wang, Y., Campbell, J. M., Poshusta, T. L., Starker, C. G., Krug, R. G., 2nd, Tan, W., Penheiter, S. G., Ma, A. C., Leung, A. Y., Fahrenkrug, S. C., Carlson, D. F., Voytas, D. F., Clark, K. J., Essner, J. J., & Ekker,

S. C. (2012). In vivo genome editing using a high-efficiency TALEN system. Nature, 491(7422), 114–118. https://doi.org/10.1038/nature11537

Bergers, G., Song, S., Meyer-Morse, N., Bergsland, E., & Hanahan, D. (2003). Benefits of targeting both pericytes and endothelial cells in the tumor vasculature with kinase inhibitors. The Journal of clinical investigation, 111(9), 1287–1295. https://doi.org/10.1172/JCI17929

Bouchet, B. P., Gough, R. E., Ammon, Y. C., van de Willige, D., Post, H., Jacquemet, G., Altelaar, A. M., Heck, A. J., Goult, B. T., & Akhmanova, A. (2016). Talin-KANK1 interaction controls the recruitment of cortical microtubule stabilizing complexes to focal adhesions. eLife, 5, e18124. https://doi.org/10.7554/eLife.18124

Burri, P. H., Hlushchuk, R., & Djonov, V. (2004). Intussusceptive angiogenesis: its emergence, its characteristics, and its significance. Developmental dynamics: an official publication of the American Association of Anatomists, 231(3), 474–488. https://doi.org/10.1002/dvdy.20184

Bussolati, B., Grange, C., Sapino, A., & Camussi, G. (2009). Endothelial cell differentiation of human breast tumour stem/progenitor cells. Journal of cellular and molecular medicine, 13(2), 309–319. https://doi.org/10.1111/j.1582-4934.2008.00338.x

Cai, J., Ahmad, S., Jiang, W. G., Huang, J., Kontos, C. D., Boulton, M., & Ahmed, A. (2003). Activation of vascular endothelial growth factor receptor-1 sustains angiogenesis and Bcl-2 expression via the phosphatidylinositol 3-kinase pathway in endothelial cells. Diabetes, 52(12), 2959–2968. https://doi.org/10.2337/diabetes.52.12.2959

Carmeliet, P., & Jain, R. K. (2011). Molecular mechanisms and clinical applications of angiogenesis. Nature, 473(7347), 298–307. https://doi.org/10.1038/nature10144

Carmeliet, P., Dor, Y., Herbert, J. M., Fukumura, D., Brusselmans, K., Dewerchin, M., Neeman, M., Bono, F., Abramovitch, R., Maxwell, P., Koch, C. J., Ratcliffe, P., Moons, L., Jain, R. K., Collen, D., & Keshert, E. (1998). Role of HIF-1alpha in hypoxia-mediated apoptosis, cell proliferation and tumour angiogenesis. Nature, 394(6692), 485–490. https://doi.org/10.1038/28867

Chávez, M. N., Aedo, G., Fierro, F. A., Allende, M. L., & Egaña, J. T. (2016). Zebrafish as an Emerging Model Organism to Study Angiogenesis in Development and Regeneration. Frontiers in physiology, 7, 56. https://doi.org/10.3389/fphys.2016.00056

Coultas, L., Chawengsaksophak, K., & Rossant, J. (2005). Endothelial cells and VEGF in vascular development. *Nature*, *438*(7070), 937–945. https://doi.org/10.1038/nature04479

Cowell, A. R., Jacquemet, G., Singh, A. K., Varela, L., Nylund, A. S., Ammon, Y. C., Brown, D. G., Akhmanova, A., Ivaska, J., & Goult, B. T. (2021). Talin rod domain-containing protein 1 (TLNRD1) is a novel actin-bundling protein which promotes filopodia formation. The Journal of cell biology, 220(9), e202005214. https://doi.org/10.1083/jcb.202005214

Cronenwett, J. L., & Johnston, K. W. (2014). Rutherford's vascular surgery (Eighth edition.). Philadelphia, PA: Saunders/Elsevier.

Cuevas, P., García-Calvo, M., Carceller, F., Reimers, D., Zazo, M., Cuevas, B., Muñoz-Willery, I., Martínez-Coso, V., Lamas, S., & Giménez-Gallego, G. (1996). Correction of hypertension by normalization of

endothelial levels of fibroblast growth factor and nitric oxide synthase in spontaneously hypertensive rats. Proceedings of the National Academy of Sciences of the United States of America, 93(21), 11996–12001. https://doi.org/10.1073/pnas.93.21.11996

Date, T., Mochizuki, S., Belanger, A. J., Yamakawa, M., Luo, Z., Vincent, K. A., Cheng, S. H., Gregory, R. J., & Jiang, C. (2005). Expression of constitutively stable hybrid hypoxia-inducible factor-1alpha protects cultured rat cardiomyocytes against simulated ischemia-reperfusion injury. American journal of physiology. Cell physiology, 288(2), C314–C320. https://doi.org/10.1152/ajpcell.00374.2004

Ding, Y., Huang, Y., Song, N., Gao, X., Yuan, S., Wang, X., Cai, H., Fu, Y., & Luo, Y. (2010). NFAT1 mediates placental growth factor-induced myelomonocytic cell recruitment via the induction of TNF-alpha. Journal of immunology (Baltimore, Md.: 1950), 184(5), 2593–2601. https://doi.org/10.4049/jimmunol.0902378

Dixelius, J., Makinen, T., Wirzenius, M., Karkkainen, M. J., Wernstedt, C., Alitalo, K., & Claesson-Welsh, L. (2003). Ligand-induced vascular endothelial growth factor receptor-3 (VEGFR-3) heterodimerization with VEGFR-2 in primary lymphatic endothelial cells regulates tyrosine phosphorylation sites. The Journal of biological chemistry, 278(42), 40973–40979. https://doi.org/10.1074/jbc.M304499200

Djonov, V., Baum, O., & Burri, P. H. (2003). Vascular remodeling by intussusceptive angiogenesis. *Cell and tissue research*, *314*(1), 107–117. https://doi.org/10.1007/s00441-003-0784-3

Drugbank (2022), "Aflibercept", last edited August 16, 2022 01:02, available at: https://go.drugbank.com/drugs/DB08885

Eklund, L., & Saharinen, P. (2013). Angiopoietin signaling in the vasculature. Experimental cell research, 319(9), 1271–1280. https://doi.org/10.1016/j.yexcr.2013.03.011

El Hallani, S., Boisselier, B., Peglion, F., Rousseau, A., Colin, C., Idbaih, A., Marie, Y., Mokhtari, K., Thomas, J. L., Eichmann, A., Delattre, J. Y., Maniotis, A. J., & Sanson, M. (2010). A new alternative mechanism in glioblastoma vascularization: tubular vasculogenic mimicry. Brain: a journal of neurology, 133(Pt 4), 973–982. https://doi.org/10.1093/brain/awq044

Elliott, P. R., Goult, B. T., Kopp, P. M., Bate, N., Grossmann, J. G., Roberts, G. C., Critchley, D. R., & Barsukov, I. L. (2010). The Structure of the talin head reveals a novel extended conformation of the FERM domain. Structure (London, England: 1993), 18(10), 1289–1299. https://doi.org/10.1016/j.str.2010.07.011

Farnsworth, D. R., Saunders, L. M., & Miller, A. C. (2020). A single-cell transcriptome atlas for zebrafish development. Developmental biology, 459(2), 100–108. https://doi.org/10.1016/j.ydbio.2019.11.008

Ferrara N. (2004). Vascular endothelial growth factor: basic science and clinical progress. Endocrine reviews, 25(4), 581–611. https://doi.org/10.1210/er.2003-0027

Ferrara, N., & Henzel, W. J. (1989). Pituitary follicular cells secrete a novel heparin-binding growth factor specific for vascular endothelial cells. Biochemical and biophysical research communications, 161(2), 851–858. https://doi.org/10.1016/0006-291x(89)92678-8

Galvagni, F., Pennacchini, S., Salameh, A., Rocchigiani, M., Neri, F., Orlandini, M., Petraglia, F., Gotta, S., Sardone, G. L., Matteucci, G., Terstappen, G. C., & Oliviero, S. (2010). Endothelial cell adhesion to the extracellular matrix induces c-Src-dependent VEGFR-3 phosphorylation without the activation of the

receptor intrinsic kinase activity. Circulation research, 106(12), 1839–1848. https://doi.org/10.1161/CIRCRESAHA.109.206326

Ge, H., & Luo, H. (2018). Overview of advances in vasculogenic mimicry - a potential target for tumor therapy. Cancer management and research, 10, 2429–2437. https://doi.org/10.2147/CMAR.S164675

Geng, L., Chaudhuri, A., Talmon, G., Wisecarver, J. L., & Wang, J. (2013). TGF-Beta suppresses VEGFA-mediated angiogenesis in colon cancer metastasis. PloS one, 8(3), e59918. https://doi.org/10.1371/journal.pone.0059918

Gingras, A. R., Lagarrigue, F., Cuevas, M. N., Valadez, A. J., Zorovich, M., McLaughlin, W., Lopez-Ramirez, M. A., Seban, N., Ley, K., Kiosses, W. B., et al. (2019). Rap1 binding and a lipid-dependent helix in talin F1 domain promote integrin activation in tandem. J. Cell Biol. 218, 1799-1809. https://doi.org/10.1083/jcb.201810061

Gong, B., Liang, D., Chew, T. G., & Ge, R. (2004). Characterization of the zebrafish vascular endothelial growth factor A gene: comparison with vegf-A genes in mammals and Fugu. Biochimica et biophysica acta, 1676(1), 33–40. https://doi.org/10.1016/j.bbaexp.2003.10.006

Goult, B. T., Zacharchenko, T., Bate, N., Tsang, R., Hey, F., Gingras, A. R., Elliott, P. R., Roberts, G., Ballestrem, C., Critchley, D. R., & Barsukov, I. L. (2013). RIAM and vinculin binding to talin are mutually exclusive and regulate adhesion assembly and turnover. The Journal of biological chemistry, 288(12), 8238–8249. https://doi.org/10.1074/jbc.M112.438119

Goult, B. T., Yan, J., & Schwartz, M. A. (2018). Talin as a mechanosensitive signaling hub. *The Journal of cell biology*, *217*(11), 3776–3784. https://doi.org/10.1083/jcb.201808061

Guschin, D. Y., Waite, A. J., Katibah, G. E., Miller, J. C., Holmes, M. C., & Rebar, E. J. (2010). A rapid and general assay for monitoring endogenous gene modification. *Methods in molecular biology (Clifton, N.J.)*, *649*, 247–256. https://doi.org/10.1007/978-1-60761-753-2_15

Hakanpaa, L., Sipila, T., Leppanen, V. M., Gautam, P., Nurmi, H., Jacquemet, G., Eklund, L., Ivaska, J., Alitalo, K., & Saharinen, P. (2015). Endothelial destabilization by angiopoietin-2 via integrin β1 activation. Nature communications, 6, 5962. https://doi.org/10.1038/ncomms6962

Hasegawa, Y., Takanashi, S., Kanehira, Y., Tsushima, T., Imai, T., & Okumura, K. (2001). Transforming growth factor-beta1 level correlates with angiogenesis, tumor progression, and prognosis in patients with nonsmall cell lung carcinoma. Cancer, 91(5), 964–971.

Heldin C. H. (2013). Targeting the PDGF signaling pathway in tumor treatment. Cell communication and signaling: CCS, 11, 97. https://doi.org/10.1186/1478-811X-11-97

Holmes, D. I., & Zachary, I. (2005). The vascular endothelial growth factor (VEGF) family: angiogenic factors in health and disease. *Genome biology*, *6*(2), 209. https://doi.org/10.1186/gb-2005-6-2-209

Hoshijima, K., Jurynec, M. J., Klatt Shaw, D., Jacobi, A. M., Behlke, M. A., & Grunwald, D. J. (2019). Highly Efficient CRISPR-Cas9-Based Methods for Generating Deletion Mutations and F0 Embryos that Lack Gene Function in Zebrafish. Developmental cell, 51(5), 645–657.e4. https://doi.org/10.1016/j.devcel.2019.10.004

Huang, K., Andersson, C., Roomans, G. M., Ito, N., & Claesson-Welsh, L. (2001). Signaling properties of VEGF receptor-1 and -2 homo- and heterodimers. The international journal of biochemistry & cell biology, 33(4), 315–324. https://doi.org/10.1016/s1357-2725(01)00019-x

Huang, L. E., Gu, J., Schau, M., & Bunn, H. F. (1998). Regulation of hypoxia-inducible factor 1alpha is mediated by an O2-dependent degradation domain via the ubiquitin-proteasome pathway. Proceedings of the National Academy of Sciences of the United States of America, 95(14), 7987–7992. https://doi.org/10.1073/pnas.95.14.7987

Isogai, S., Lawson, N. D., Torrealday, S., Horiguchi, M., & Weinstein, B. M. (2003). Angiogenic network formation in the developing vertebrate trunk. Development (Cambridge, England), 130(21), 5281–5290. https://doi.org/10.1242/dev.00733

Itoh, N., & Ornitz, D. M. (2004). Evolution of the Fgf and Fgfr gene families. Trends in genetics: TIG, 20(11), 563–569. https://doi.org/10.1016/j.tig.2004.08.007

Jahani, M., Rezazadeh, D., Mohammadi, P., Abdolmaleki, A., Norooznezhad, A., & Mansouri, K. (2020). Regenerative Medicine and Angiogenesis; Challenges and Opportunities. Advanced pharmaceutical bulletin, 10(4), 490–501. https://doi.org/10.34172/apb.2020.061

Jarad, M., Kuczynski, E. A., Morrison, J., Viloria-Petit, A. M., & Coomber, B. L. (2017). Release of endothelial cell associated VEGFR2 during TGF-β modulated angiogenesis in vitro. BMC cell biology, 18(1), 10. https://doi.org/10.1186/s12860-017-0127-y

Kaipainen, A., Korhonen, J., Mustonen, T., van Hinsbergh, V. W., Fang, G. H., Dumont, D., Breitman, M., & Alitalo, K. (1995). Expression of the fms-like tyrosine kinase 4 gene becomes restricted to lymphatic endothelium during development. Proceedings of the National Academy of Sciences of the United States of America, 92(8), 3566–3570. https://doi.org/10.1073/pnas.92.8.3566

Kanno, S., Oda, N., Abe, M., Terai, Y., Ito, M., Shitara, K., Tabayashi, K., Shibuya, M., & Sato, Y. (2000). Roles of two VEGF receptors, Flt-1 and KDR, in the signal transduction of VEGF effects in human vascular endothelial cells. Oncogene, 19(17), 2138–2146. https://doi.org/10.1038/sj.onc.1203533

Kharitonenkov, A., Shiyanova, T. L., Koester, A., Ford, A. M., Micanovic, R., Galbreath, E. J., Sandusky, G. E., Hammond, L. J., Moyers, J. S., Owens, R. A., Gromada, J., Brozinick, J. T., Hawkins, E. D., Wroblewski, V. J., Li, D. S., Mehrbod, F., Jaskunas, S. R., & Shanafelt, A. B. (2005). FGF-21 as a novel metabolic regulator. The Journal of clinical investigation, 115(6), 1627–1635. https://doi.org/10.1172/JCI23606

Khurana, S., & George, S. P. (2011). The role of actin bundling proteins in the assembly of filopodia in epithelial cells. Cell adhesion & migration, 5(5), 409–420. https://doi.org/10.4161/cam.5.5.17644

Kido, M., Du, L., Sullivan, C. C., Li, X., Deutsch, R., Jamieson, S. W., & Thistlethwaite, P. A. (2005). Hypoxia-inducible factor 1-alpha reduces infarction and attenuates progression of cardiac dysfunction after myocardial infarction in the mouse. Journal of the American College of Cardiology, 46(11), 2116–2124. https://doi.org/10.1016/j.jacc.2005.08.045

Klint, P., & Claesson-Welsh, L. (1999). Signal transduction by fibroblast growth factor receptors. Frontiers in bioscience: a journal and virtual library, 4, D165–D177. https://doi.org/10.2741/klint

Klint, P., Kanda, S., Kloog, Y., & Claesson-Welsh, L. (1999). Contribution of Src and Ras pathways in FGF-2 induced endothelial cell differentiation. Oncogene, 18(22), 3354–3364. https://doi.org/10.1038/sj.onc.1202680

Koch, S., Tugues, S., Li, X., Gualandi, L., & Claesson-Welsh, L. (2011). Signal transduction by vascular endothelial growth factor receptors. The Biochemical journal, 437(2), 169–183. https://doi.org/10.1042/BJ20110301

Krock, B. L., Skuli, N., & Simon, M. C. (2011). Hypoxia-induced angiogenesis: good and evil. Genes & cancer, 2(12), 1117–1133. https://doi.org/10.1177/1947601911423654

Kuijper, S., Turner, C. J., & Adams, R. H. (2007). Regulation of angiogenesis by Eph-ephrin interactions. Trends in cardiovascular medicine, 17(5), 145–151. https://doi.org/10.1016/j.tcm.2007.03.003

Kulla, A., Burkhardt, K., Meyer-Puttlitz, B., Teesalu, T., Asser, T., Wiestler, O. D., & Becker, A. J. (2003). Analysis of the TP53 gene in laser-microdissected glioblastoma vasculature. Acta neuropathologica, 105(4), 328–332. https://doi.org/10.1007/s00401-003-0681-6

Lando, D., Peet, D. J., Whelan, D. A., Gorman, J. J., & Whitelaw, M. L. (2002). Asparagine hydroxylation of the HIF transactivation domain a hypoxic switch. Science (New York, N.Y.), 295(5556), 858–861. https://doi.org/10.1126/science.1068592

Larsson, H., Klint, P., Landgren, E., & Claesson-Welsh, L. (1999). Fibroblast growth factor receptor-1-mediated endothelial cell proliferation is dependent on the Src homology (SH) 2/SH3 domain-containing adaptor protein Crk. The Journal of biological chemistry, 274(36), 25726–25734. https://doi.org/10.1074/jbc.274.36.25726

Lebrin, F., Srun, S., Raymond, K., Martin, S., van den Brink, S., Freitas, C., Bréant, C., Mathivet, T., Larrivée, B., Thomas, J. L., Arthur, H. M., Westermann, C. J., Disch, F., Mager, J. J., Snijder, R. J., Eichmann, A., & Mummery, C. L. (2010). Thalidomide stimulates vessel maturation and reduces epistaxis in individuals with hereditary hemorrhagic telangiectasia. Nature medicine, 16(4), 420–428. https://doi.org/10.1038/nm.2131

Lee, J., Kim, K. E., Choi, D. K., Jang, J. Y., Jung, J. J., Kiyonari, H., Shioi, G., Chang, W., Suda, T., Mochizuki, N., Nakaoka, Y., Komuro, I., Yoo, O. J., & Koh, G. Y. (2013). Angiopoietin-1 guides directional angiogenesis through integrin αvβ5 signaling for recovery of ischemic retinopathy. Science translational medicine, 5(203), 203ra127. https://doi.org/10.1126/scitranslmed.3006666

Li, J., Zhang, Y. P., & Kirsner, R. S. (2003). Angiogenesis in wound repair: angiogenic growth factors and the extracellular matrix. Microscopy research and technique, 60(1), 107–114. https://doi.org/10.1002/jemt.10249

Liu, S., Chen, S., & Zeng, J. (2018). TGF-β signaling: A complex role in tumorigenesis (Review). Molecular medicine reports, 17(1), 699–704. https://doi.org/10.3892/mmr.2017.7970

Lugano, R., Ramachandran, M., & Dimberg, A. (2020). Tumor angiogenesis: causes, consequences, challenges and opportunities. Cellular and molecular life sciences: CMLS, 77(9), 1745–1770. https://doi.org/10.1007/s00018-019-03351-7

Luo, Q., Wang, J., Zhao, W., Peng, Z., Liu, X., Li, B., Zhang, H., Shan, B., Zhang, C., & Duan, C. (2020). Vasculogenic mimicry in carcinogenesis and clinical applications. Journal of hematology & oncology, 13(1), 19. https://doi.org/10.1186/s13045-020-00858-6

Makanya, A. N., Hlushchuk, R., & Djonov, V. G. (2009). Intussusceptive angiogenesis and its role in vascular morphogenesis, patterning, and remodeling. Angiogenesis, 12(2), 113–123. https://doi.org/10.1007/s10456-009-9129-5

Mammoto, T., Jiang, A., Jiang, E., & Mammoto, A. (2016). Role of Twist1 Phosphorylation in Angiogenesis and Pulmonary Fibrosis. American journal of respiratory cell and molecular biology, 55(5), 633–644. https://doi.org/10.1165/rcmb.2016-0012OC

Maniotis, A. J., Chen, X., Garcia, C., DeChristopher, P. J., Wu, D., Pe'er, J., & Folberg, R. (2002). Control of melanoma morphogenesis, endothelial survival, and perfusion by extracellular matrix. Laboratory investigation; a journal of technical methods and pathology, 82(8), 1031–1043. https://doi.org/10.1097/01.lab.0000024362.12721.67

Maniotis, A. J., Folberg, R., Hess, A., Seftor, E. A., Gardner, L. M., Pe'er, J., Trent, J. M., Meltzer, P. S., & Hendrix, M. J. (1999). Vascular channel formation by human melanoma cells in vivo and in vitro: vasculogenic mimicry. The American journal of pathology, 155(3), 739–752. https://doi.org/10.1016/S0002-9440(10)65173-5

Massagué J. (1998). TGF-beta signal transduction. Annual review of biochemistry, 67, 753–791. https://doi.org/10.1146/annurev.biochem.67.1.753

Meeker, N. D., Hutchinson, S. A., Ho, L., & Trede, N. S. (2007). Method for isolation of PCR-ready genomic DNA from zebrafish tissues. *BioTechniques*, *43*(5), 610–614. https://doi.org/10.2144/000112619

Meshel, A. S., Wei, Q., Adelstein, R. S., & Sheetz, M. P. (2005). Basic mechanism of three-dimensional collagen fibre transport by fibroblasts. Nature cell biology, 7(2), 157–164. https://doi.org/10.1038/ncb1216

Mohammadi, M., Honegger, A. M., Rotin, D., Fischer, R., Bellot, F., Li, W., Dionne, C. A., Jaye, M., Rubinstein, M., & Schlessinger, J. (1991). A tyrosine-phosphorylated carboxy-terminal peptide of the fibroblast growth factor receptor (Flg) is a binding site for the SH2 domain of phospholipase C-gamma 1. *Molecular and cellular biology*, *11*(10), 5068–5078. https://doi.org/10.1128/mcb.11.10.5068-5078.1991

Mäkinen, T., Veikkola, T., Mustjoki, S., Karpanen, T., Catimel, B., Nice, E. C., Wise, L., Mercer, A., Kowalski, H., Kerjaschki, D., Stacker, S. A., Achen, M. G., & Alitalo, K. (2001). Isolated lymphatic endothelial cells transduce growth, survival and migratory signals via the VEGF-C/D receptor VEGFR-3. The EMBO journal, 20(17), 4762–4773. https://doi.org/10.1093/emboj/20.17.4762

National Institute of Health, National Cancer Institute (2018): “Angiogenesis inhibitors”, U.S. Department of Health and Human Services, National Institutes of Health, National Cancer Institute, USA.gov, available at: https://www.cancer.gov/about-cancer/treatment/types/immunotherapy/angiogenesis-inhibitors-fact-sheet

Neufeld, G., Cohen, T., Gengrinovitch, S., & Poltorak, Z. (1999). Vascular endothelial growth factor (VEGF) and its receptors. FASEB journal: official publication of the Federation of American Societies for Experimental Biology, 13(1), 9–22.

Ogawa, S., Oku, A., Sawano, A., Yamaguchi, S., Yazaki, Y., & Shibuya, M. (1998). A novel type of vascular endothelial growth factor, VEGF-E (NZ-7 VEGF), preferentially utilizes KDR/Flk-1 receptor and carries a potent mitotic activity without heparin-binding domain. *The Journal of biological chemistry*, *273*(47), 31273–31282. https://doi.org/10.1074/jbc.273.47.31273

Olsen, J. J., Pohl, S. Ö., Deshmukh, A., Visweswaran, M., Ward, N. C., Arfuso, F., Agostino, M., & Dharmarajan, A. (2017). The Role of Wnt Signalling in Angiogenesis. The Clinical biochemist. Reviews, 38(3), 131–142.

Pagé, E. L., Robitaille, G. A., Pouysségur, J., & Richard, D. E. (2002). Induction of hypoxia-inducible factor-1alpha by transcriptional and translational mechanisms. The Journal of biological chemistry, 277(50), 48403–48409. https://doi.org/10.1074/jbc.M209114200

Paku, S., Dezso, K., Bugyik, E., Tóvári, J., Tímár, J., Nagy, P., Laszlo, V., Klepetko, W., & Döme, B. (2011). A new mechanism for pillar formation during tumor-induced intussusceptive angiogenesis: inverse sprouting. The American journal of pathology, 179(3), 1573–1585. https://doi.org/10.1016/j.ajpath.2011.05.033

Peach, C. J., Mignone, V. W., Arruda, M. A., Alcobia, D. C., Hill, S. J., Kilpatrick, L. E., & Woolard, J. (2018). Molecular Pharmacology of VEGF-A Isoforms: Binding and Signalling at VEGFR2. International journal of molecular sciences, 19(4), 1264. https://doi.org/10.3390/ijms19041264

Phng, L. K., Stanchi, F., & Gerhardt, H. (2013). Filopodia are dispensable for endothelial tip cell guidance. *Development (Cambridge, England)*, *140*(19), 4031–4040. https://doi.org/10.1242/dev.097352

Potente, M., Gerhardt, H., & Carmeliet, P. (2011). Basic and therapeutic aspects of angiogenesis. Cell, 146(6), 873–887. https://doi.org/10.1016/j.cell.2011.08.039

Pugsley, M. K., & Tabrizchi, R. (2000). The vascular system. An overview of structure and function. Journal of pharmacological and toxicological methods, 44(2), 333–340. https://doi.org/10.1016/s1056-8719(00)00125-8

Rahikainen, R., von Essen, M., Schaefer, M., Qi, L., Azizi, L., Conor, K., Kelly, C., Ihalainen, T. O., Wehrle-Haller, B., Martin, B., Bastmeyer, M., Cai, H., Huang, C., & Hytönen, V. P. (2017). Mechanical stability of talin rod controls cell migration and substrate sensing. Scientific reports, 7(1), 3571. [3571]. https://doi.org/10.1038/s41598-017-03335-2

Ricci-Vitiani, L., Pallini, R., Biffoni, M., Todaro, M., Invernici, G., Cenci, T., Maira, G., Parati, E. A., Stassi, G., Larocca, L. M., & De Maria, R. (2010). Tumour vascularization via endothelial differentiation of glioblastoma stem-like cells. Nature, 468(7325), 824–828. https://doi.org/10.1038/nature09557

Risau W. (1997). Mechanisms of angiogenesis. Nature, 386(6626), 671–674. https://doi.org/10.1038/386671a0

Rodriguez, F. J., Scheithauer, B. W., Giannini, C., Bryant, S. C., & Jenkins, R. B. (2008). Epithelial and pseudoepithelial differentiation in glioblastoma and gliosarcoma: a comparative morphologic and molecular genetic study. Cancer, 113(10), 2779–2789. https://doi.org/10.1002/cncr.23899

Ruzicka, L., Bradford, Y. M., Frazer, K., Howe, D. G., Paddock, H., Ramachandran, S., Singer, A., Toro, S., Van Slyke, C. E., Eagle, A. E., Fashena, D., Kalita, P., Knight, J., Mani, P., Martin, R., Moxon, S. A., Pich, C., Schaper,

K., Shao, X., & Westerfield, M. (2015). ZFIN, The zebrafish model organism database: Updates and new directions. Genesis (New York, N.Y. : 2000), 53(8), 498–509. https://doi.org/10.1002/dvg.22868

Saharinen, P., Eklund, L., Miettinen, J., Wirkkala, R., Anisimov, A., Winderlich, M., Nottebaum, A., Vestweber, D., Deutsch, U., Koh, G. Y., Olsen, B. R., & Alitalo, K. (2008). Angiopoietins assemble distinct Tie2 signalling complexes in endothelial cell-cell and cell-matrix contacts. Nature cell biology, 10(5), 527–537. https://doi.org/10.1038/ncb1715

Sánchez-Elsner, T., Botella, L. M., Velasco, B., Corbí, A., Attisano, L., & Bernabéu, C. (2001). Synergistic cooperation between hypoxia and transforming growth factor-beta pathways on human vascular endothelial growth factor gene expression. The Journal of biological chemistry, 276(42), 38527–38535. https://doi.org/10.1074/jbc.M104536200

Schmidt, A., Brixius, K., & Bloch, W. (2007). Endothelial precursor cell migration during vasculogenesis. Circulation research, 101(2), 125–136. https://doi.org/10.1161/CIRCRESAHA.107.148932

Shimotake, J., Derugin, N., Wendland, M., Vexler, Z. S., & Ferriero, D. M. (2010). Vascular endothelial growth factor receptor-2 inhibition promotes cell death and limits endothelial cell proliferation in a neonatal rodent model of stroke. Stroke, 41(2), 343–349. https://doi.org/10.1161/STROKEAHA.109.564229

Sun, Z., Li, X., Massena, S., Kutschera, S., Padhan, N., Gualandi, L., Sundvold-Gjerstad, V., Gustafsson, K., Choy, W. W., Zang, G., Quach, M., Jansson, L., Phillipson, M., Abid, M. R., Spurkland, A., & Claesson-Welsh, L. (2012). VEGFR2 induces c-Src signaling and vascular permeability in vivo via the adaptor protein TSAd. The Journal of experimental medicine, 209(7), 1363–1377. https://doi.org/10.1084/jem.20111343

Takahashi, T., Yamaguchi, S., Chida, K., & Shibuya, M. (2001). A single autophosphorylation site on KDR/Flk-1 is essential for VEGF-A-dependent activation of PLC-gamma and DNA synthesis in vascular endothelial cells. The EMBO journal, 20(11), 2768–2778. https://doi.org/10.1093/emboj/20.11.2768

Tammela, T., Zarkada, G., Wallgard, E., Murtomäki, A., Suchting, S., Wirzenius, M., Waltari, M., Hellström, M., Schomber, T., Peltonen, R., Freitas, C., Duarte, A., Isoniemi, H., Laakkonen, P., Christofori, G., Ylä-Herttuala, S., Shibuya, M., Pytowski, B., Eichmann, A., Betsholtz, C., … Alitalo, K. (2008). Blocking VEGFR-3 suppresses angiogenic sprouting and vascular network formation. Nature, 454(7204), 656–660. https://doi.org/10.1038/nature07083

Tatarano, S., Chiyomaru, T., Kawakami, K., Enokida, H., Yoshino, H., Hidaka, H., Nohata, N., Yamasaki, T., Gotanda, T., Tachiwada, T., Seki, N., & Nakagawa, M. (2012). Novel oncogenic function of mesoderm development candidate 1 and its regulation by MiR-574-3p in bladder cancer cell lines. International journal of oncology, 40(4), 951–959. https://doi.org/10.3892/ijo.2011.1294

Taylor AM, Bordoni B. Histology, Blood Vascular System. [Updated 2022 May 8]. In: StatPearls [Internet]. Treasure Island (FL): StatPearls Publishing; 2022 Jan-. Available from: https://www.ncbi.nlm.nih.gov/books/NBK553217/

Tchaikovski V., Fellbrich G., Waltenberger J. The molecular basis of VEGFR-1 signal transduction pathways in primary human monocytes. Arterioscler, Thromb. Vasc. Biol., 2008, vol. 28 (pg. 322-328) Available from: https://www.ahajournals.org/doi/10.1161/ATVBAHA.107.158022

Tucker WD, Arora Y, Mahajan K. Anatomy, Blood Vessels. [Updated 2021 Aug 11]. In: StatPearls [Internet]. Treasure Island (FL): StatPearls Publishing; 2022 Jan-. Available from: https://www.ncbi.nlm.nih.gov/books/NBK470401/

Udan, R. S., Culver, J. C., & Dickinson, M. E. (2013). Understanding vascular development. Wiley interdisciplinary reviews. Developmental biology, 2(3), 327–346. https://doi.org/10.1002/wdev.91

Wang Y, Zhao S. Vascular Biology of the Placenta. San Rafael (CA): Morgan & Claypool Life Sciences; 2010. Chapter 6, Vasculogenesis and Angiogenesis of Human Placenta. Available from: https://www.ncbi.nlm.nih.gov/books/NBK53252/

Welti, J., Loges, S., Dimmeler, S., & Carmeliet, P. (2013). Recent molecular discoveries in angiogenesis and antiangiogenic therapies in cancer. The Journal of clinical investigation, 123(8), 3190–3200. https://doi.org/10.1172/JCI70212

Wong, V. W., & Crawford, J. D. (2013). Vasculogenic cytokines in wound healing. BioMed research international, 2013, 190486. https://doi.org/10.1155/2013/190486

Yamazaki, Y., Matsunaga, Y., Tokunaga, Y., Obayashi, S., Saito, M., & Morita, T. (2009). Snake venom Vascular Endothelial Growth Factors (VEGF-Fs) exclusively vary their structures and functions among species. The Journal of biological chemistry, 284(15), 9885–9891. https://doi.org/10.1074/jbc.M809071200

Yang, J., Zhu, L., Zhang, H., Hirbawi, J., Fukuda, K., Dwivedi, P., Liu, J., Byzova, T., Plow, E. F., Wu, J., & Qin, J. (2014). Conformational activation of talin by RIAM triggers integrin-mediated cell adhesion. Nature communications, 5, 5880. https://doi.org/10.1038/ncomms6880

Yang, Y., Xie, P., Opatowsky, Y., & Schlessinger, J. (2010). Direct contacts between extracellular membrane-proximal domains are required for VEGF receptor activation and cell signaling. Proceedings of the National Academy of Sciences of the United States of America, 107(5), 1906–1911. https://doi.org/10.1073/pnas.0914052107

Yu, Q., & Stamenkovic, I. (2000). Cell surface-localized matrix metalloproteinase-9 proteolytically activates TGF-beta and promotes tumor invasion and angiogenesis. Genes & development, 14(2), 163–176.

Zhao, Y., Bao, Q., Renner, A., Camaj, P., Eichhorn, M., Ischenko, I., Angele, M., Kleespies, A., Jauch, K. W., & Bruns, C. (2011). Cancer stem cells and angiogenesis. The International journal of developmental biology, 55(4-5), 477–482. https://doi.org/10.1387/ijdb.103225yz